Vietnam National Universities – HCMC
International University
Biomedical Engineering Department

A DIGITAL MICROFLUIDICS (DMF) SYSTEM FOR POINT-OF-CARE (POC) NUCLEIC ACID AMPLIFICATION TESTS (NAAT)

by

Hoang Trung Thien

A thesis submitted to the Biomedical Engineering Department in partial fulfillment of the requirements for the degree of Engineer

Ho Chi Minh City, Vietnam

July-2018

Vietnam National Universities – HCMC
International University
Biomedical Engineering Department

A DIGITAL MICROFLUIDICS (DMF) SYSTEM FOR POINT-OF-CARE (POC) NUCLEIC ACID AMPLIFICATION TESTS (NAAT)

Huynh Chan Khon, PhD., Advisor

, PhD., Reviewer

APPROVED BY:

Prof. Võ Văn Tới, PhD., Chair

, PhD.

, PhD.

, PhD., Secretary

THESIS COMMITTEE

ACKNOWLEGEMENTS

Foremost, I would like to send my greatest gratitude to my academic advisor, Dr. Huỳnh Chấn Khôn for his for her valuable and constructive suggestions and guidance during the planning and development of this research work. His motivation, enthusiasm and immense knowledge have helped me a lot to accomplish this project in the most comprehensive manner.

My grateful thank is also extended to the Department of Biomedical Engineering of the International University, especially Prof. Võ Văn Tới, who has continually conveyed a spirit of adventure in regard of learning and making innovations in my academic work.

I would also like to express my deep gratitude to Msc. Nguyễn Thanh Tâm and Mr. Nguyễn Hoàng Tuấn for their helpful advice so that I could overcome all difficulties while finalizing this project.

Special thanks to my friends Le Thanh Xuan and Nguyen Le Y, for their unconditional love and support. They have supported me to the best of their abilities through useful research experience they share and all memorable lab work sessions through late nights that we have spent together during this project . It is such a great pleasure for me to know them.

Last but not least, I wish to express my love and gratitude to my beloved family for their understanding and invaluable encouragement throughout the whole research process. My parents are my inspiration and motivation. I could not have accomplished everything without their love. This work is dedicated to all the individuals who love and support me.

Vietnam National Universities – HCMC
International University
Biomedical Engineering Department

TABLE OF CONTENTS

LIST OF FIGURES

LIST OF ABBREVIATIONS

AC	Alternating Current
BSA	Bovine Serum Albumin
CNC	Computer Numerical Control
DC	Direct Current
DIY	Do It Yourself
DMF	Digital Microfluidics
DNA	Deoxyribonucleic Acid
EW	Electrowetting
EWOD	Electrowetting – on – dielectric
ITO	Indium Tin Oxide
LAMP	Loop-mediated isothermal Amplification
µTAS	Micro Total Analysis Systems
NAAT	Nucleic Acid Amplification Test
PCB	Printed circuit board
PCR	Polymerase Chain Reaction
PDMS	Polydimethylsiloxane
POC	Point – of – care
PVDF	Polyvinylidene difluoride
RNA	Ribonucleic Acid
RPA	Recombinase Polymerase Amplification
SAW	Surface Acoustics Wave
WHO	World Health Organization

ABSTRACT

Recently, Digital Microfluidics (DMF) has been recognized as a promising candidate for the next generation of point-of-care diagnostic devices. Especially, when combined with molecular biology techniques such as Nucleic Acid Amplification Tests (NAATs), it can allow accurate and robust but simple, rapid and field-compatible molecular diagnostics of various pathogens and conditions. The aim of this research is to conduct an investigation on the design and fabrication of a such DMF system, intentionally used for detection of infectious diseases in Vietnam by NAATs. The system works based on the principle of electrowetting-on-dielectric (EWOD) effect, which is a technique to control the motion of individual microscale to nanoscale liquid droplets using the electric force. The presented DMF system was constructed from four main components, including a controller board integrated with a high-voltage power converter, an electrode panel fabricated by the PCB industry, a foil carrier used for carrying the insulating layer and finally, an ITO glass slide as the top counter electrode. PDMS was chosen as the insulating material because of its inexpensiveness and availability. Peanut oil was used as a lubricant to reduce contact angle hysteresis of PDMS surface due to the incompatibility with other organic oils of PDMS. Using a 275V, 1kHz driving signal, the current DMF device was verified to be capable of performing four basic droplet operations including droplet dispense, droplet transportation, droplet mixing and droplet splitting, even though further investigation is mandatory for a more quantitative control of droplet volume. Moreover, the device was able to work with droplets of protein solutions, which was not possible in the pre-thesis work. A Recombinase Polymerase Amplification (RPA) assay was also designed to run on the presented device; however, the experiment failed to complete because the

high viscosity of the RPA Master mix exceeded the actuation limit of the current system. In this thesis research, the performance of the DMF device is limited mainly due to the use of inappropriate materials. However, the results from this research did provide more understanding into the field of Digital Microfluidics and the lessons learned from the failures can be premises for further development and improvements in the next design.

Keywords: *Digital microfluidics, EWOD, PDMS, NAATs*

CHAPTER I: INTRODUCTION

1.1. Background and Motivation

Recent years have seen the emergence of an interdisciplinary research to develop miniaturized and integrated chemical and biological analysis systems, which are commonly known as lab-on-a-chip or micro total analysis systems (μTAS). The goal of developing these systems stems from the need to reduce common bio- and chemical-laboratory procedures and equipment to miniaturized, automated formats, thereby enabling rapid, portable, inexpensive and reliable instrumentation with applications in medical diagnostics, drug discovery, environmental monitoring and basic scientific research. The high-throughput and dramatically reduced reagent consumption and labor requirements of the lab-on-a-chip systems also enable certain techniques which would normally be prohibitively expensive or time-consuming by conventional methods. Thus, the lab-on-a-chip research has the potential not only to enhance but to transform many areas of science and medicine.

The lab-on-a-chip systems crucially depend on the microfluidics, which is the study and manipulation of minute quantities of liquids. Conventional microfluidics technology uses micro-channels and other mechanical components such as pump and valve to control the continuous flow of liquids. Despite its explicit benefits of minimal reagent consumption and faster time-to-result, this type of microfluidics still lacks of automation and re-configurability, i.e. the capability of addressing a reasonably wide range of problems with a single design. This raises a need for another solution which is

based upon the manipulation and control of discrete fluid units – the Digital Microfluidics.

Digital Microfluidics (or DMF in short) is an emerging technology in the field of microfluidics that is capable of manipulating individual, microscale (µL) to nanoscale (nL) liquid droplets on a planner surface [1]. Possessing not only all standard benefits offered by the channel-based microfluidics, namely volume reduction, increased volume-to-surface ratio, therefore, faster reaction rate, increased process sensitivity and decrease in sample cross-contamination, the DMF technology also comes with salient features that are not present in the conventional microfluidics such as no channels or mechanical parts required for droplet propulsion, highly reconfigurable and programmable droplet control for different procedures, scalability, portability and automation-readiness [2][3][4][5]. Thanks to those superior features, DMF can fit in a wide range of applications including chemical and enzymatic reactions, proteomics, immunoassays, DNA-based applications and particularly, point-of-care diagnostics.

Nucleic acid amplification tests (NAAT) is one of the most relevant tools in molecular biology by which a small amount of plant nucleotide fragments (RNA or DNA sequences) can be duplicated exponentially to produce more samples to be detected. By allowing the identification and characterization of signature nucleic acid sequences, the technique plays a key element in molecular diagnostics of various health problems such as cancer, hereditary conditions, infectious pathogens and also in the detection of antimicrobial resistance[2][6] , which is an uprising challenge for the current healthcare system and puts human lives in dangers again with common infectious diseases that used to be curable by antimicrobial drugs [7].

The combination of nucleic acid amplification test onto a DMF system has been explored through several research and numerous advantages have been pointed out. The chemical consumption could be reduced up to 40,000-fold [8], and the detection limit has been improved up to 100 times [9] compared to bench-top processes. The reaction time was reported to drop by 50% [10] and fully automatic and multiplexing processes, can further cut down on costs and cross-contamination risks. With those results, DMF-based nucleic acid amplification test is a potential tool for the future point-of-care (POC) diagnostics and helps shift the paradigm of molecular diagnostics from the centralized structure of highly specialized laboratories to local diagnostics close to patients' place.

In recent years, molecular biology has made a remarkable breakthrough in clinical diagnostics in Vietnam by allowing the detection of dangerous pathogens such as HIV, syphilis, hepatitis B and C or dengue fever, from early stages when the symptoms have not manifested yet and therefore, screening by conventional methods is not effective. However, the accessibility of patients to molecular biology testing is still limited by two major difficulties: technology limitation and high cost. This method requires healthcare facilities to be equipped with modern machinery and high technical level staffs, that typically present only at centralized hospitals in big cities while rural areas are the ones to be more vulnerable to infections. This raised a urgent need for a solution to tackle that problem, for example, a molecular diagnostic device based on digital microfluidics technology that is portable and inexpensive, not only dedicated to Vietnam but also suitable for other developing countries with similar situations.

1.2. Objective and Scope

The goal of this research is to investigate the design and fabrication of a digital microfluidic (DMF) system which can be used with nucleic acid amplification tests (NAAT). In fact, this research field is not new, however, it is suitable and helpful for situations in Vietnam, as well as other developing countries. The research is conducted with a hope to enable point-of-care molecular diagnostics at epidemic sites and minimize the expense of each test performed. The scope of this research is attempting to obtain the objective by using the easily accessible and readily available materials and equipment, due to our limited budgets, for the fabrication process of the device.

In this research, the digital microfluidic system was fabricated entirely on PCB panels and PDMS thin membrane was used for both the dielectric and hydrophobic layers. There are several reasons why PDMS was an attractive selection. Firstly, PDMS is an inexpensive and commonly available material in the field of microfluidics, which can be easily processed into a thin membrane by spin coating. This property is suitable for our laboratory conditions due to our limited access to microfabrication processes that are commonly used for dielectric layer deposition. Secondly, PDMS has a moderate dielectric constant of 2.7 [11] and very good hydrophobicity, which can be used for both purposes, dielectric and hydrophobic layers, with a single layer deposited. Despite have much better performance than PDMS, more common materials for hydrophobic coating such as Teflon AF1600 or Cytop were not used in this research because they are relatively expensive and their use are usually limited by licensing agreements with the Company for both research and commercial purposes. Thin PDMS membranes were selected instead of directly spin-coating PDMS onto electrodes in order to avoid

unwanted dielectric breakdown, which usually occurs in the gap between electrodes due to uneven coating and to better control the thickness of the layer. With this selection, we have encountered two significant problems including the minimum thickness of PDMS coatings (which should have enough dielectric strength to withstand a high electric field while being as thin as possible to minimize the required actuation voltage) and the high contact hysteresis of PDMS surface which often hinders droplet motion [12][13]. Peanut oil and AC driving signal had been utilized to lower the threshold voltage and overcome the effect of high contact angle hysteresis. The use of silicone oil, as extensively reported in literature, or other organic oils were not satisfactory since those oils can penetrate and damage the thin PDMS layer. Nevertheless, the high viscosity of peanut oil, as compared to silicone oil, has an adverse effect on the speed of droplet movements by increasing the resistance force. As a consequence, even though the DMF system presented in this thesis report was verified to be capable of performing all four basic operations on droplets, its actuation performance was not as good as expected and therefore, running more complicated experiments on the device is not ready yet.

1.3. Organization of report

The remain of this thesis report is organized as follows:

Chapter II: covers literature review on micro-actuating technologies that have been investigated for liquid droplet manipulation. This chapter also considers the design and operation of a typical digital microfluidic (DMF) system based on the Electrowetting-on-dielectric (EWOD) effect.

Chapter III: states the research methodology including a brief description of all materials and equipment used in the research, the construction and fabrication process of the presented DMF system and an experimental study on the capacity of the fabricated device to perform droplet operations which are fundamental for any chemical and biological protocols.

Chapter IV: displays the results of those experiments described in chapter III.

Chapter V: provides discussions on mentioned results and proposes possible directions for future works.

Chapter VI: covers the conclusion of this research work.

CHAPTER II: LITERATURE REVIEW

2.1. Surface tension and wettability

A surface can be either hydrophilic (contact angle < 90°) or hydrophobic (contact angle > 90°) [14][15], as illustrated in Figure 1. If we drop a liquid onto a flat, horizontal solid surface, the three interfacial tensions, including solid-vapor, solid-liquid, and liquid-vapor interfacial tensions, operate together at the three-phase contact line to maintain the droplet equilibrium at a certain contact angle. The relation between the contact angle θ and the interfacial tensions can be expressed by the Young's equation [14][16][17] as:

$$\cos\theta = \frac{\gamma_{SV} - \gamma_{SL}}{\gamma_{LV}} \quad (1)$$

where γ_{SV}, γ_{SL} and γ_{LV} are the solid-vapor, solid-liquid, and liquid-vapor interfacial tensions respectively.

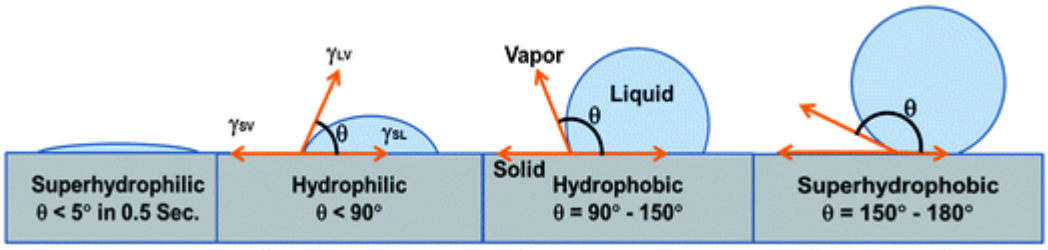

Figure 1: Contact angle of liquid droplets on surfaces with different wettability [74]

2.2. Surface tension – based methods for driving droplets

When it comes to liquid droplets of sub-millimeter dimensions, surface tension becomes the dominant force acting in the systems. It has been speculated that "if human beings were creatures of sub-millimeter in size, the main force of interest to us would have been surface tension, many machines would be driven by surface-

tension- based motors, while inertia would be just an interesting but unimportant force"[18]. If in continuous-flow systems, surface tension usually appears as an unwelcome force which resists the filling of channels or dislodgement of air bubbles. In digital microfluidics, in contrast, surface tension should be viewed as the target force for micro-actuation and therefore, active modulation of surface tension is preferably chosen as an important strategy for the fluid control.

Actuation of droplets by surface tension force typically relies on the surface tension gradients to drive the bulk flow of liquid droplets on solid surfaces and requires a method to actively control at least one of the three interfacial energies co-existing at the three-phase contact line. Over a few past decades, researchers have explored different driving mechanisms for actuation of droplets, such as chemical effects [13] [14], photochemical effect [20], thermocapillary effect [21]–[24], surface acoustics wave (SAW) [25]–[29], magnetic forces [30]–[33], dielectrophoretic methods [34], continuous electrowetting [30][31], electrowetting and electrowetting – on – dielectric (EWOD) [17], [37]–[41]. Among these techniques, the surface tension modulation at the solid – liquid interface is the most popular because of the site-specific control and localization of surface forces at micro-scale, resulting in more flexible, scalable and simpler systems to design and operate. Specifically, the modulation of surface tension by electrically-driven mechanisms attract more attention mainly because of their lesser power consumption and heat dissipation. Especially, the EWOD technique, which uses the modification of wettability of liquid droplets on a solid insulating surface via electric potential, is very much promising due to the chemical inertness of the surface and no suffering from electrolysis decomposition as in the EW method.

2.3. EWOD – based Digital Microfluidics

Consider a conducting droplet resting on a non-wetting solid insulator of thickness d and relative dielectric constant ε_r, as illustrated in Figure 2(a). When an external voltage V is applied between the wire touching the droplet and the counter electrode underneath, surface charges accumulated on the insulating layer will reduce the effective surface tension between the droplet and the solid surface so that

$$\gamma_{SL}(V) = \gamma_{SL}(0) - \frac{\varepsilon_0 \varepsilon_r}{2d} V^2 \qquad (2)$$

which is essentially the equation originally derived by Lippman (Appendix of [16]), the first to discover the electrocapillary effect, for the mercury – electrolyte interface. By substituting this equation in the Young's equation of contact angle (Eq.1), we obtain

$$\cos\theta(V) = \cos\theta_0 + \frac{\varepsilon_0 \varepsilon_r}{2d\gamma_{LV}} V^2 \qquad (3)$$

where θ is the equilibrium contact angle at the applied voltage V and θ_0 is the contact angle at zero potential (V = 0), ε_0 is the permittivity of vacuum, ε_r is the relative dielectric constant of the dielectric layer and d is its thickness. This equation is named as the Young – Lippman equation and is considered as the basic equation for the electrowetting – on – dielectric (EWOD) effect, by which the contact angle of the droplet decreases under the application of an external electric potential. This EWOD technique is different from another similar but distinct technique known as electrowetting (EW) by the fact that EWOD has a thin insulating layer [42] , which is absent in the precedentially developed EW technique, to avoid direct contact between the droplet and the electrode underneath, and therefore, electrolysis decomposition can be eliminated as long as this insulating layer does not break down.

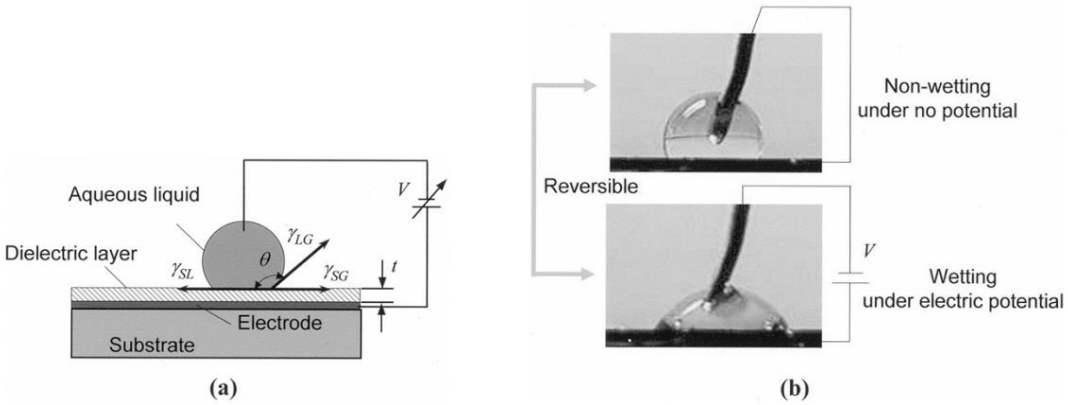

Figure 2: Principle of electrowetting – on – dielectric (EWOD) [17]
(a) Schematic configuration. (b) EWOD effect demonstration (volume ~ 5uL)

As described above, the EWOD technique provides a mechanism for actuation of droplets via the voltage – control of the solid – liquid interfacial tension. An asymmetric change in the interfacial tension induces an asymmetric deformation of the droplet menisci, resulting in a pressure gradient between two ends of the droplet that gives rise to bulk fluid movement (black arrow in the figure below). It is essential that the footprint of the droplet to be controlled should overlap two adjacent electrodes to enable the effect. Figure 3 reports the droplet movement principle for both configurations of EWOD – based actuation of droplets. It is necessary to emphasize that this approach is correct to explain the macroscopic effect of droplet movement and is useful for practical applications of EWOD-based actuation. However, there have been still some deviations from ideality where the EWOD approach fails to explain the liquid dielectrophoretic force, which is predominant at high frequencies spectrum of the applied electric potential or for dielectric liquids [40][41]. A more direct and generalized understanding of the force that drives droplets may be thoroughly explained by other models such as the electromechanical model [45].

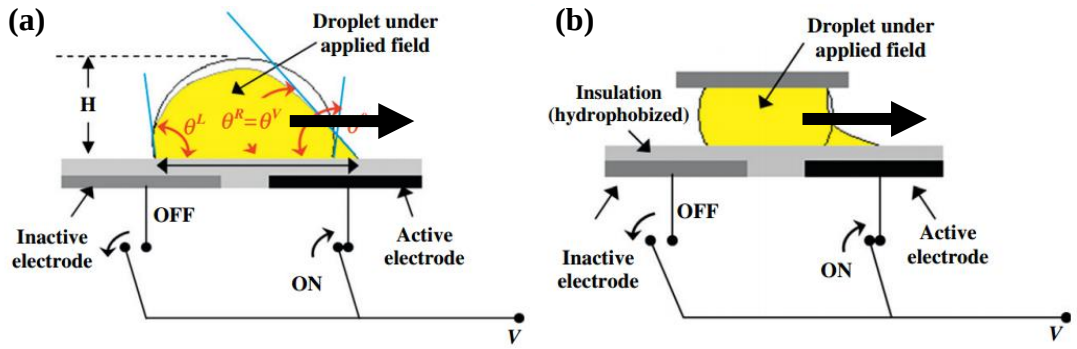

Figure 3: EWOD actuation principle in [64]

(a) Open configuration (b) Closed configuration

EWOD-based digital microfluidics devices usually operate, using two different configurations [46][47][48][49]: open or single-plate and closed or dual-plate configurations. In the open configuration, the droplet is placed on a single plate consisting of a substrate, usually glass deposited with patterned electrodes and coated with a stacked structure of dielectric and hydrophobic layers. The electrode array controls the movement path of droplets, the dielectric layer supports the electric field required for EWOD effect and avoid electrolysis while the hydrophobic layer facilitates the variation in contact angle and enables facile droplet movement. The advantages of this configuration include direct access to droplets (for analysis and so forth) [47], capacity to move large droplets with small footprints and enhanced mixing effect compared to closed configuration [50][51]. The drawback of this configuration is that it only supports droplet transportation and droplet mixing operations. Figure 4(a) shows the cross-section of the open configuration. On the other hand, the closed configuration in which droplets will be sandwiched between two plates, the top and bottom plate is the more popular configuration used owing to its capacity to perform additional droplet dispense from a reservoir and droplet splitting compared to the former configuration [17][40]. In this configuration, the bottom plate is identical to the one used in the open configuration while the top plate usually uses an unpatterned conductive layer deposited

on a piece of glass as a counter-electrode (usually ITO, Indium-Tin-Oxide, glass is used). A hydrophobic layer is also added to the top plate to enable droplet motion. The top and bottom plates are separated by some spacers and the gap between them may be filled with an immiscible fluid such as silicone oil or left with air [37] depending on applications. Even though air medium is more suitable for a wider range of applications such as cell culture [52]–[54] or manipulation of oil-miscible liquids, it is reported that filler oil can significantly reduce the threshold voltage, which is the minimum voltage required for droplet movement, and contact angle hysteresis of the surface (the higher the contact angle hysteresis, the more difficult to move a droplet), which results in a much easier droplet motion. Immiscible fluid fillers also help prevent droplet evaporation and biofouling [1][16][55][56], which is the adsorption of biomolecules/ proteins onto hydrophobic surfaces and renders the droplets immovable on the DMF device. Some successful examples with not only DNA and proteins samples but also physiological fluids such as whole blood, plasma and urine were reported in [2]–[4][57][58]. The cross-section of closed configuration is illustrated in Figure 4(b).

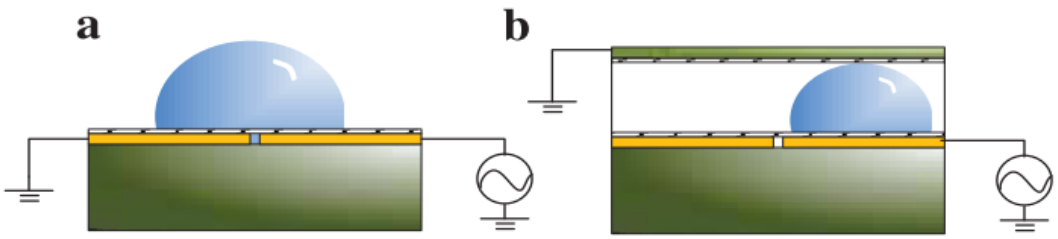

Figure 4: Cross-section of (a) Open configuration (b) Closed configuration [46]

For most applications, the digital microfluidic chip or the electrode array for simplicity is fabricated using standard microfabrication techniques such as metal deposition on glass slides followed by photolithography and wet etching for electrodes and electrical connections patterning, deposition of thermal growth of dielectric layer

and deposition of hydrophobic layer, usually by spin coating. These processes usually have the advantages of high resolution, thin and uniform layers formation and therefore, great integration into a monolithic device with multi-layers of structures. However, the drawbacks of microfabrication techniques are that they usually require clean room conditions and very expensive equipment and machinery. One more disadvantage of using microfabrication processes to fabricate the electrodes onto glass slides is that when the number of electrodes rises, electrical wiring becomes a problem. Therefore, there have been several research on using the PCB (printed circuit board) as the substrate for electrode arrays [38][49], taking advantages of mature and low-cost PCB industry that is capable of manufacturing circuits with multiple separate wiring layers, which can be electrically accessed through drilled vias with copper-electroplated inner walls. This helps tackle the problem of wiring when the number of electrodes grow enormous. The downside of this method is the surface topography and roughness of PCB that resulted in high resistance against droplet motion and as a consequence, required a much higher actuation voltage (~ 500V). Compared to electrode pads on glass slides (thickness of 100 – 200nm and inter-electrode gap of 4-10µm), electrodes fabricated on PCB substrate has much thicker Cu layer and wider inter-electrode gap (25µm and 75 µm, respectively [60]) due to limits of PCB technology. This not only hinders the droplet motion but also causes difficulties in the deposition of the insulating layer. A remedy to those problems was provided in [60] where three refined PCB microfabrication processes were proposed. Even though the results were that droplets could be moved in air with a lower voltage (~ 80VAC), those post-PCB processes were still complicated and depends on microfabrication techniques. In this thesis research, another simpler method was used to overcome similar problems. A free-standing

polymer film can be applied on the top of the electrodes, providing both the insulating layer and a smoother surface for droplet movements. Similar methods were also previously reported in [5][51]. This approach also provides a way to save the cost of electrode panel when the dielectric and the hydrophobic layers are degraded, which can happens often under the pressure of high actuation voltage.

The insulating layer, unlike other components of an EWOD-based device, is the most crucial and has remarkable impacts on the device performance [16][55]. From the basic equation of EWOD (Eq.3), two main criteria for fabricating this layer are suggested that firstly, the contact angle of liquid droplets without applied voltage should be as large as possible, in order to obtain a maximum contact angle variation ($\Delta \cos \theta$), and secondly the insulating layer should have as high dielectric constant and be as thin as possible to minimize the electric potential required for actuation. In most applications, the insulating layer of a EWOD-based device consists of two layers, the dielectric layer and the hydrophobic layer, even though there was a circumstance that a single-layer insulator could be used [13]. The dielectric layer sustains the electric field generated by the electric potential and can be fabricated using either polymer materials such as Parylene [49][40][37][62], Teflon [63] or PDMS [48][49][13] or inorganic materials such as SiO_2 [17][64], SiN[55], BST (Barium Strontium Titanate) [62]. The hydrophobic layer is coated on top of the dielectric layer and provides liquid droplets with a large initial contact angle, normally above 100^o, and low resistive surface. Usually Teflon AF1600 or more recently Cytop is used for this coating. In fact, Teflon AF1600 is the most common material for hydrophobic coating in literature due to its highly hydrophobicity (contact angle of 120^o [55]) and low contact angle hysteresis (9^o in air and 2^o in silicone oil [13]). While polymer materials offer a simpler fabrication

process such as spin coating, inorganic materials have an advantage of lower actuating voltage thanks to their higher dielectric constants, described by the equation (4) below:

$$V\ (\Delta \cos\theta) = \sqrt[2]{\frac{2\ d\ \gamma_{lg}(\cos\theta_0 - \cos\theta)}{\varepsilon_0 \varepsilon_r}} \qquad (4)$$

Minimizing the insulator thickness can reduce the required electric potential (see equation (4)); however, dielectric break down of this layer may result if the dielectric strength of the material is not enough. The commonly used polymer materials usually have much lower dielectric strength than the inorganic dielectrics [55] (except for BST used in [62]). The minimum thickness of the insulating layer is determined by both the threshold voltage for droplet actuation and the breakdown voltage of the material used. In total, ideally, the insulating layer of an EWOD-based system should have a high dielectric constant and enough/high dielectric strength to withstand the electric potential used. In addition, the materials should be chemically inert, mechanically durable and highly stable to ensure reproducibility and long life-time [16][55]. In some cases, Saran wrap (cling wrap or food wrap) and commercial water repellant solution (Rain-X, for example) can also be used for fast prototyping purpose [46][47][5].

Although electric potential used for EWOD-based actuation of droplets can be either DC (direct current) or AC (alternating current) , it was reported that AC driving signal outperformed the DC one by exhibiting no hysteresis, which is caused by the charge-trapping effect and can result in unreliable droplet control, and less risk of insulator degradation while experiences only minimal increases in threshold voltage at higher frequencies [65]. Other drawbacks of the AC actuation method includes less compatibility with electronic components and the requirement for dedicated and more

expensive components such as photo-MOSFET to handle the AC driving signal. Systems using AC driving signal, therefore, usually have bigger footprint than the ones operating with DC actuation signal [66].

2.4. EWOD – based Digital Microfluidics for Nucleic acid amplification

Various research applying the principle of EWOD into DMF-based nucleic acid amplification tests (NAATs) have been conducted. A few example designs of such systems are shown below. In Figure 5(a) is the DMF platform that was developed by the Chang group [10] for the purpose of amplifying a detection gene for the Dengue II virus using the PCR (polymerase chain reaction) technique – the gold standard of NAAT [2]. Figure 5(b) is another example of a DMF platform that was designed for loop-mediated isothermal amplification (LAMP) test of Trypanosoma brucei DNA [4].

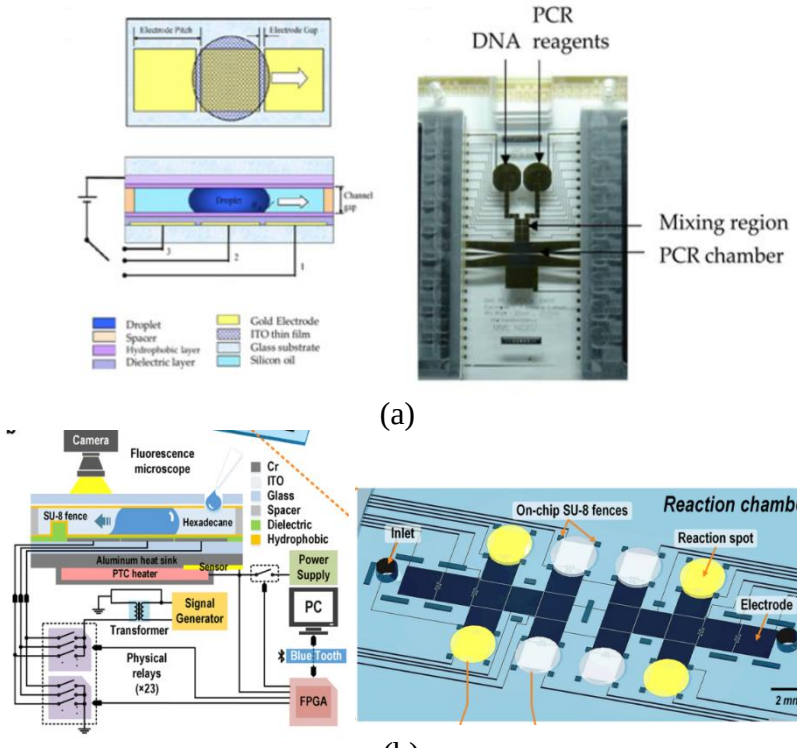

Figure 5: Example designs of DMF system for (a) PCR (b) LAMP

CHAPTER III: METHODOLOGY

3.1. Materials & Equipment

The digital microfluidic chips with the electrode array design used in this research were fabricated on standard FR4 substrates of the PCB industry (specifications of which include thickness of copper: 1oz ~ 35µm; thickness of substrate: 1.6mm) and was manufactured by the PCBzonevn (Nam Ky Khoi Nghia street, Binh Duong Province, Vietnam). Other PCB designs were fabricated by another local manufacturer KimsonPCB (Nguyen Thi Minh Khai street, District 1, Ho Chi Minh City, Vietnam) due to their less intricate design. The electronic components used in the research were purchased from various sources such as Digikey (USA), taobao.com (China) or thegioiic (Vietnam). All of the PCB designing work was accomplished using the Eagle PCB software (Autodesk, student license).

Sylgard 184 Silicone kit (Dow Corning, USA) was selected as the material for PDMS membrane. Other materials used in the fabrication process of the device included Indium-Tin-Oxide (ITO) coated glass slide (Luoyang Guluo Glass .Ltd, China) and peanut oil (Tuong An, Vietnam) which was bought from local supermarket.

Chemicals used for device testing experiments included 50X TAE solution and protein BSA (Bovine Serum Albumin). For the RPA experiment, the TwistAmp® Liquid Basic kit was purchased from TwistDx Ltd. (Cambridge, United Kingdom). The food-coloring dye was purchased from the local supermarket.

3.2. Fabrication Process

3.2.1. Digital microfluidic (DMF) device

The presented DMF system consists of four main components:

A controller board integrated with a high voltage power converter which is capable of stepping up to 275VDC from a 12VDC input. This power converter was originally designed for the application of powering Nixie tubes [67] and was also adapted to provide an adjustable voltage up to 260V for a digital microfluidic platform in [5]. This power converter design was selected in the present work instead of an external high-voltage lab-bench power supply because of its ready integration ability for fully automated digital microfluidic platform in the future. The power converter design used for this device allows the digital microfluidic platform to be powered directly from a common wall socket with a 12V adapter and offers the user the option to adjust the voltage up to 275VDC by rotating the potentiometer using a screwdriver.

At the heart of the controller board is an Arduino Nano, the function of which is to manipulate status, either on or off, of appropriate electrodes to facilitate continuous movement of droplets of liquids. The micro-controller is also responsible for bi-directional communication between the DMF device and a PC user interface from which energized status of electrodes can be viewed and controlled using keyboards.

A 64-channel and 300V-rating serial to parallel shift register, namely HV507 (from Microchip Technology Inc.), played as an intermediate between the 5V-compatible micro-controller and high voltage power line. The HV507 is a low voltage serial to high voltage parallel converter with 64 push-pull outputs, allowing control of an array of up to 64 electrodes using a single 80-pin IC package (Datasheet available at

[68]). This feature makes it a potential component to be selected for the integrated and fully automated digital microfluidic platform in the future, which will be capable of controlling a larger two dimensional (2D) matrix of electrodes and offer a high variety in applications.

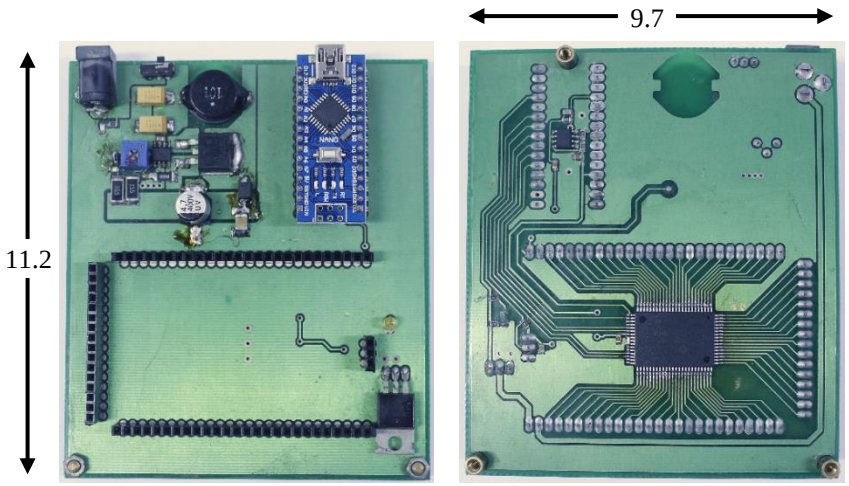

Figure 6: Top view (left) and bottom view (right) of the controller board. Board dimensions are 11.2 cm x 9.7 cm

An electrode board consisting of 63 usable electrodes (55 actuating electrodes of 3x3 mm and 8 reservoirs of 6x5mm in dimensions) was fabricated on a piece of standard FR4 substrate of the PCB industry. The inter-electrode gap was kept at 4 mil or approximately 100µm which was already the lower limit of the current PCB fabrication technology. Inter-digitated fingers were added to the electrode design, as illustrated in Figure 3, so that continuous movement of droplets could be achievable [3][8] even though it was also pointed out that the inter-digitated design may not really be necessary [11]. The electrode array board was designed to be mounted directly onto the controller board via arrays of header connector and could be easily replaced with another board. This feature originated from the thought of having a way that the DMF system can work with disposable chips in order to minimize cross-contamination risks between tests and save costs from replacing the entire device with a new one.

A foil carrier that is used as a frame for holding fragile and easy-to-wrinkle PDMS membranes while the membranes were placed upon the electrode array. In this study, the foil carrier was made out of a low-grade PCB substrate cut by a mini CNC machine and etched in Ferric Chloride solution until copper was completely removed.

The top electrode was a conductive Indium-Tin-Oxide (ITO) glass slide coated with PDMS for a hydrophobic surface. The transparency of the ITO glass slide allows the observation of droplet behaviors during operations. Double-sided copper tape was used to provide electrical connection to the top electrode.

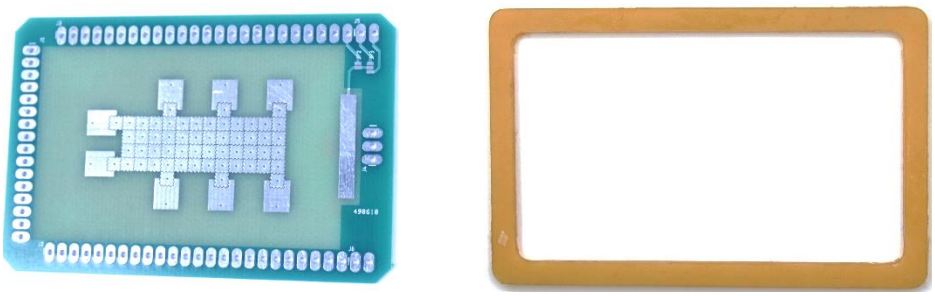

Figure 7: The electrode board (left) and the foil carrier (right)

3.2.2. Dielectric and hydrophobic layer

Thin PDMS membranes used in this research were prepared by spinning PDMS emulsion on the backsides of polystyrene Petri dishes [69] with a home-made spin coater (Appendix 1). The Sylgard 184 Elastomer Kit from Dow Corning, USA (dielectric constant ~ 2.7 [11]) was selected as the PDMS to be used in this work. The emulsion was prepared by mixing a 10 to 1 ratio of base to curing agent with a magnetic stirrer in 10 minutes. The mixture was then placed in a vacuum desiccator to remove air bubbles. Several attempts might be needed before a clear and free-of-bubble mixture could be obtained. PDMS membranes were spin-coated at 3000rpm, 150s and cured in

an oven at 50°C – 60°C in 2 hours. Higher temperature can speed up the curing process but may damage the Petri dish. After being completely cured, PDMS membranes were peeled off the Petri dish backside with a pre-made PDMS ring and uncured PDMS as glue. The foil carrier was then attached to the membrane, and the foil was cut out with a scalpel. The top electrode of the device was also spin-coated with PDMS at 3000rpm in 30 minutes. Three pieces of electrical tape (127µm thick each) were used to separate two plates. A few drops of peanut oil were dispensed and evenly spread onto the top of the electrode array in prior to applying the membrane to ensure the adherence to the electrode surface and help repel air bubbles that might be trapped between the membrane and the electrodes. Thanks to the intrinsic hydrophobicity of PDMS surface, no additional hydrophobic treatment was required in the process. Peanut oil was filled into the space between two plates to lubricate the surface and prevent droplet evaporation. Droplets could be introduced into the system by manual pipetting before the top plate was installed or via unit-size droplet dispense operation.

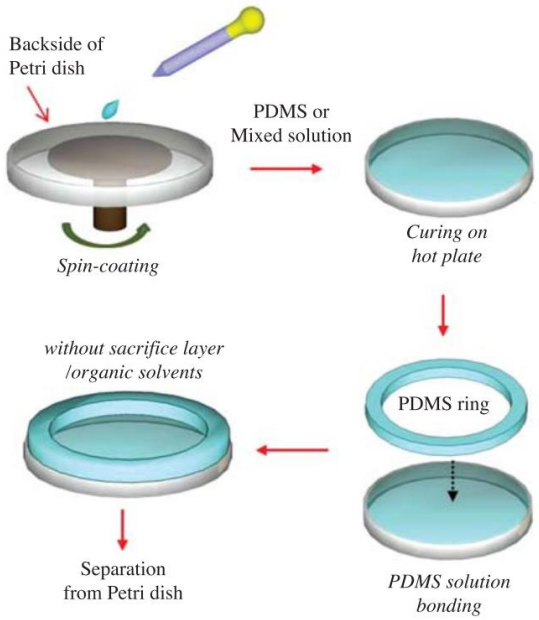

Figure 8: Fabrication process of the thin PDMS membrane [69]

3.2.3. Integrated heating unit

Because nucleic acid amplification tests normally requires temperature as an operating condition, a design of a heating unit was also integrated underneath the electrode panel of this DMF system. The heating unit was constructed from a thin-film heating element adhered to the bottom side of the electrode panel by double-coated tissue tape (9448A, 3M) as the thermal conductive layer. A DS18B20 digital temperature sensor, attached directly to the heating element also by the 3M double-sided tissue tape, reads and feedbacks the temperature to the Arduino Nano. A PID (Proportional – Integral – Derivatives) algorithm, coefficients of which were tuned in the Matlab PID tuner, was employed to regulate the temperature by turning on/off a MOSFET. Because what the temperature sensor actually reads is the temperature of the heating element itself which is generally deviated from the temperature liquid droplets will experience due to several-layer separation, a Fluke True RMS V Digital Multimeter and a 80BK K-type thermocouple probe were used to monitor the real temperatures of a peanut oil layer above the electrode panel with a PDMS membrane in between (See more in Appendices). This method provides a way to investigate and calibrate the heating unit so that the surface temperature can be achieved as accurate as possible.

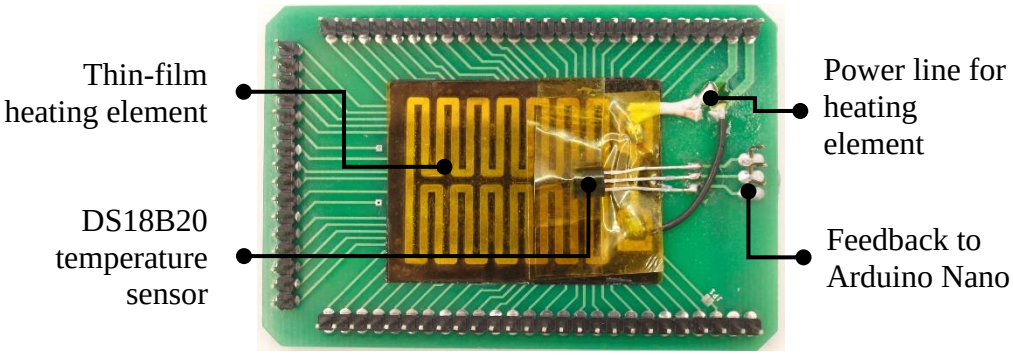

Figure 9: Heating unit integrated underneath the electrode panel. Black is the color of the double-coated tissue tape used to enhance thermal conduction.

3.2.4. Actuating configurations

In this thesis report, the performance of both DC and AC electric potentials were experimented. The purpose of that was to investigate and confirm the advantages of the AC electric potential. Figure 10 describes the connection diagram of the reported DMF system, where one output of the high-voltage shift register (the 64th in the figure) was connected to the top electrode while leaving the rest 63 outputs connected to actuating electrodes on the bottom substrate. In the DC configuration, the top electrode of the DMF device was always kept grounded (in order words, at 0V) while the electrodes underneath were activated by being connected to high voltage level, i.e. 275VDC. An inverse version of the above DC configuration was also examined in order to determine a better way of actuating droplets. In this set-up, the top electrode of the DMF device was always connected to high voltage level (275VDC) while the electrodes at the bottom plate would be activated by being grounded. The same method was previously reported in my pre-thesis work and other literature [5][48]. Figure 10(a) and 10(b) below describe the two DC configurations mentioned above. The third configuration experimented on the DMF system used an AC electric potential. A square wave (on/off) signal generated from a digital pin on the Arduino Nano was sent to the polarity pin (POL for abbreviation, negatively triggered) of the shift register and caused the register to alter its output polarities (on turns into off and vice versa), thus creating an AC actuating signal between the top plate and the bottom plate [15]. An illustration of this configuration is provided in Figure 10(c).

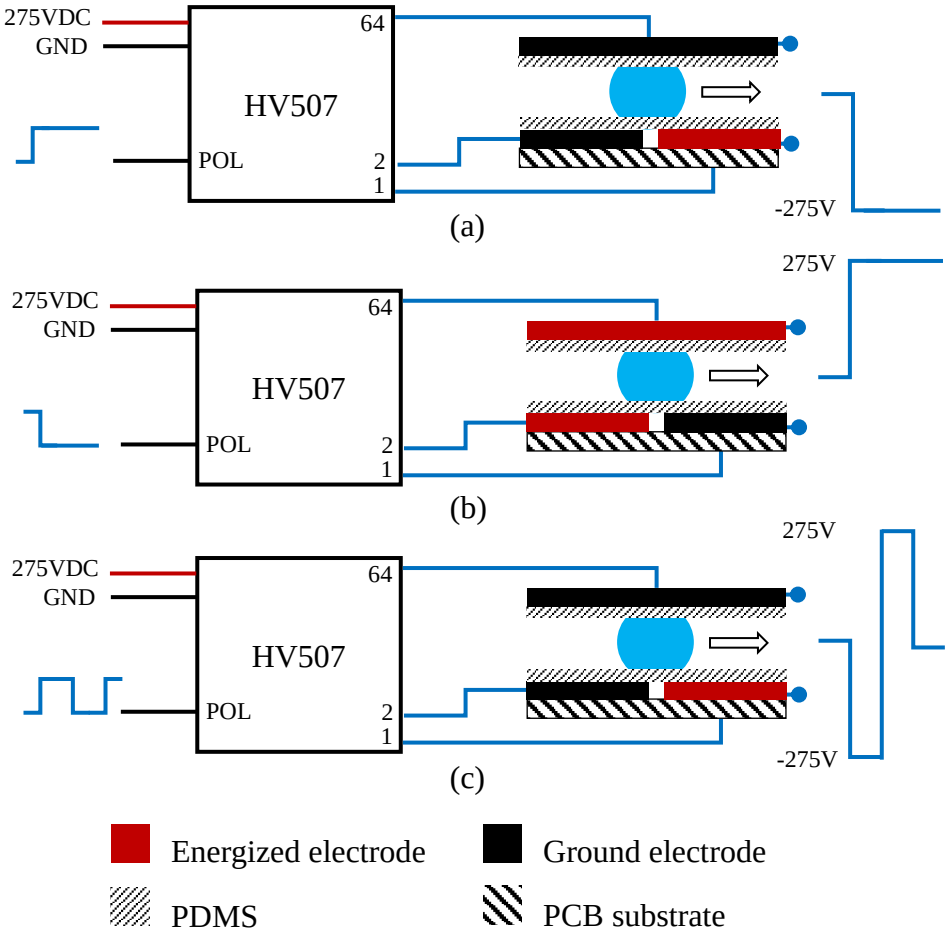

Figure 10: Electrical connection diagram for (a) DC configuration (b) inverse DC configuration (c) AC configuration

3.3. Experimental set-ups

3.3.1. PDMS membrane thickness measurement

Thickness of PDMS membranes was measured by the Scanning Electron Microscope (SEM) (SEM and Cell Culture Laboratory, Department of Biomedical Engineering, International University, VNU-HCMC)

3.3.2. Contact Angle measurement

The hydrophobicity of the PDMS membranes was characterized by measuring contact angles of sessile 10µL water droplets sitting on the membranes. A

Canon EOS 650D DSLR camera with an 18-55mm kit lens was used to take images of water droplets lying on the PDMS surface. These images were then input into the ImageJ (a free-license image processing software) and contact angle values were estimated using the Contact Angle plug-in. Figure 11 shows the setup for contact angle measurement.

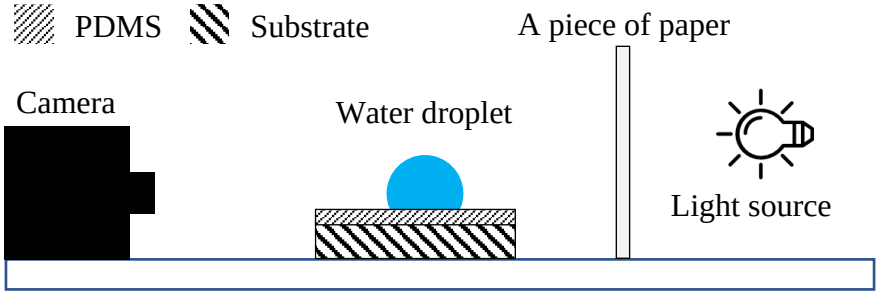

Figure 11: Experimental setup for contact angle measurements.

3.3.3. AC & DC comparison

A comparison was conducted to investigate the difference in actuation effect between the AC and DC electric potentials. Droplets of 50X TAE solution mixed with red food dye was dispensed onto the electrode array and each configuration (DC, inverse DC or AC) took turns to transport the droplets. Switching between configurations could be done with a user interface running in the Windows environment. The performance of each configuration was evaluated according to the continuity and the speed of droplet movement. Results were recorded by a digital microscope.

3.3.4. Droplet operations

Droplets of 50X TAE solution mixed with different food-coloring dyes were used to verify the capacity of the system to perform basic droplet operations comprising: *transport*, *mixing*, *splitting* and *dispense*. These experiments were

accomplished using the AC actuation signal (275V, 1kHz) because of its out-performance over DC ones. A simple Windows application was developed to provide a user interface from which status of actuating electrodes could be controlled manually via keyboards. A digital microscope was used to observe and record results during experiments.

Droplet transportation. Droplets of 50X TAE solution mixed with red food dye, after being dispensed from the reservoir, were transported over a number of electrodes and in multiple directions by the DMF device. The threshold actuation voltage and the change in droplet speed according to applied voltage values were also identified in this experiment.

Droplet dispense. A volume of 20µL of 50X TAE solution mixed with red food dye was pipetted onto an energized reservoir where the droplet would be sucked into the space between two plates by the electrowetting effect. Then, a liquid protrusion or finger connected to the liquid reservoir was created by turning on a path of electrodes adjacent to the source. Once the liquid finger extended across all energized electrodes, the intermediate electrode was grounded while the terminal and reservoir electrodes were maintained energized, causing the liquid finger to break at that location and a new droplet to be formed on the terminal energized electrode.

Droplet mixing. Two droplets of 50X TAE solution dyed with different colors (blue and yellow in this experiment) were first brought together and merged. Mixing was performed by actuating two adjacent electrodes at a time, known as double actuation in this report, in order to handle a larger droplet. The merged droplet was circulated in a loop pattern to speed up mixing, taking advantage of recirculating flow inside droplets during transportation.

Droplet splitting. After being merged and mixed, the combined droplet was split back into two smaller droplets by sequentially energizing the electrodes on either side while keeping an electrode underneath turned on. The splitting sequence was conducted in both linear path and diagonal path in the experiment and the difference in results was observed.

3.3.5. Actuation of protein droplets

In order to verify if the use of an immiscible medium filler, such as peanut oil in this study, can really suppress the adsorption of proteins onto hydrophobic surfaces, droplets of BSA protein solution at three different concentrations (5 $mg.mL^{-1}$, 2.5 $mg.mL^{-1}$ and 1.25 $mg.mL^{-1}$) were tested with dispense and transportation operations. The ability to prevent biofouling phenomenon of peanut oil was estimated based on whether droplets of protein solution could be transported without occlusion. The experiment was carried out using the same 275V, 1kHz driving signal and the results were recorded by a digital microscope.

3.3.6. DMF-based Recombinase Polymerase Amplification (RPA)

RPA is a highly sensitive and rapid isothermal amplification technique that is suitable for use on simple diagnostic devices, in low-resource settings or at point-of-need. Compared to the loop-mediated isothermal amplification (LAMP), RPA has the advantages of lower operating temperature (37^o – 42^o compared to 60^o – 65^o in LAMP) and fewer number of primers required (2 primers compared to 4-6 primers). Overall, RPA is an ideal candidate for rapid and field-compatible diagnostic platforms, like the DMF system that had been fabricated and investigated in this study.

Because of its simplicity and isothermal operating condition, RPA was selected to be tested on the presented DMF system. In a collaboration with Ms. Le Thanh Xuan, an RPA experiment was designed to run on the DMF device using 10.5µL of Master mix and 3.5µL of a solution containing DNA and Magnesium Acetate pre-mixed at a 1:3 ratio. The Master mix, consisting of 2x reaction buffer, dNTPs, 10x Basic E-Mix, a primer pair and 20x Core Reaction Mix, was prepared in advance by Ms. Le Thanh Xuan. Due to insufficient amount of the reagents we have, dispensing droplets from reservoirs filled with large volume was not possible but manual pipetting of required volumes had to be exploited. The top electrode was shifted to one side so that the first actuating electrodes after reservoirs on the other side could be reached (see Figure 12 below). One 3.5µL of DNA and Magnesium Acetate mixture would be dispensed directly on one electrode while three other droplets of Master mix was planned to be input, one by one, from the next position. The DNA and Magnesium Acetate droplet would then be transported towards and mixed with three Master mix droplets, one after one, to finally create a mixture of 1:3 ratio. An incubation temperature of 40^{o}C (+ 1.1^{o}C/ - 1.9^{o}C) was obtained by the integrated heating unit introduced above. The results were recorded by an external DLSR camera.

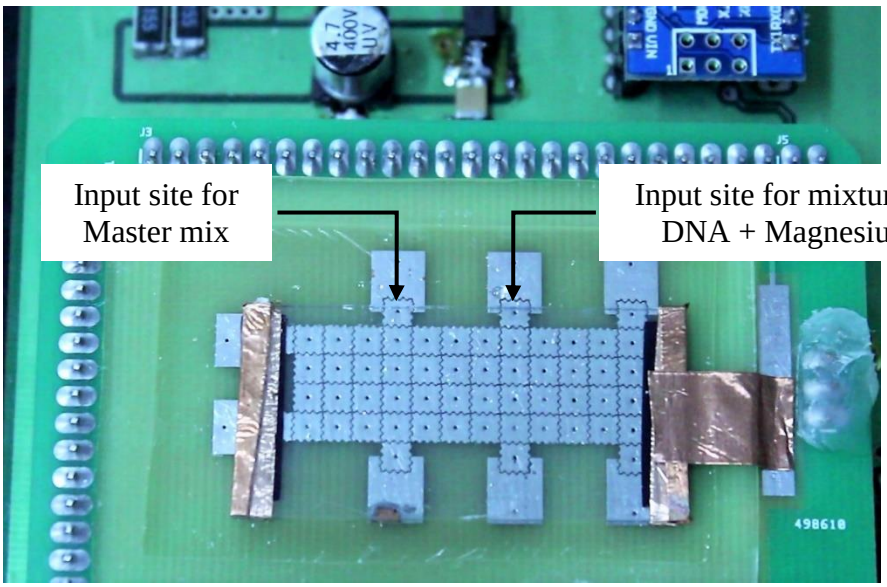

Figure 12: RPA experiment design on DMF system. The top electrode had to be shifted downwards so that first actuating electrodes after reservoirs on the upper side could be reached for manual droplet dispense by pipettes.

CHAPTER IV: RESULTS

4.1. Digital microfluidic (DMF) system

Figure 13 displays the top view of the digital microfluidic (DMF) device implemented in this research with all of its components indicated.

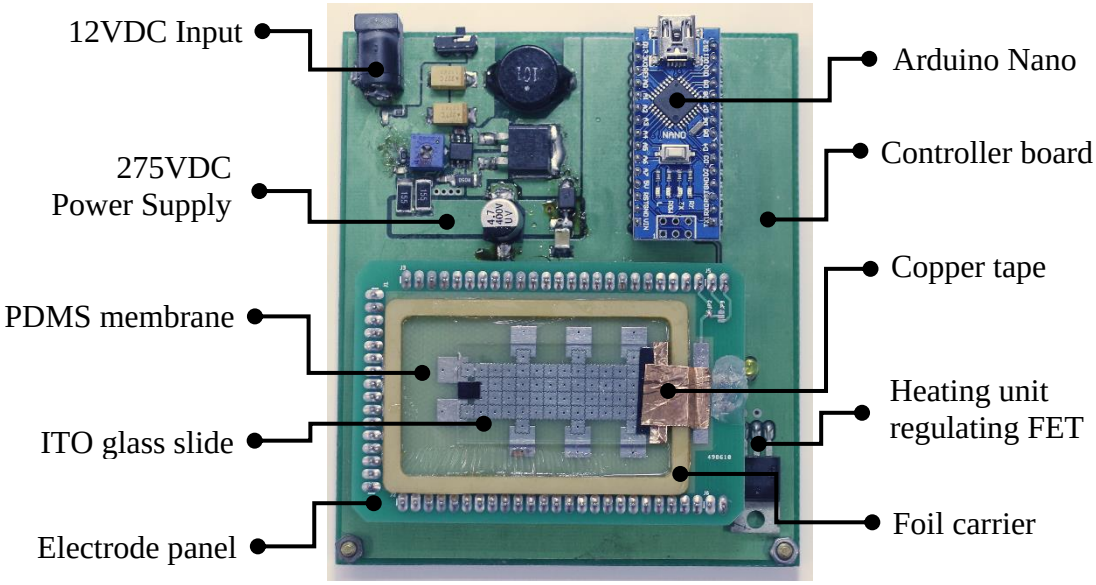

Figure 13: Top view of the Digital Microfluidic (DMF) system.

The controller board with the integrated high-voltage power converter is at the bottom and serves as the base of the device. The electrode array is mounted onto the controller using arrays of header connector. A foil carrier made of low-grade PCB substrate carries a PDMS membrane onto the top of the electrodes with a few drops of peanut oil spread between them. An ITO glass slide coated with PDMS for hydrophobic surface is placed on top of PDMS membrane. Two layers are separated from each other by three pieces of black electrical tape (127µm thick each). The top electrode is connected to a copper pad for electrical connection by double-sided copper tape. Peanut oil is used as the medium filler for the space between the top and the bottom plates.

4.2. PDMS membrane characterization

The SEM measurement reveals the thickness of the spin-coated PDMS membrane to be approximately 11.85µm (± 0.67µm). This value of thickness is the average of ten measurements along the membrane. Figure 14 below shows a PDMS membrane just separated from the petri dish with a PDMS ring and its SEM image with ten thickness values.

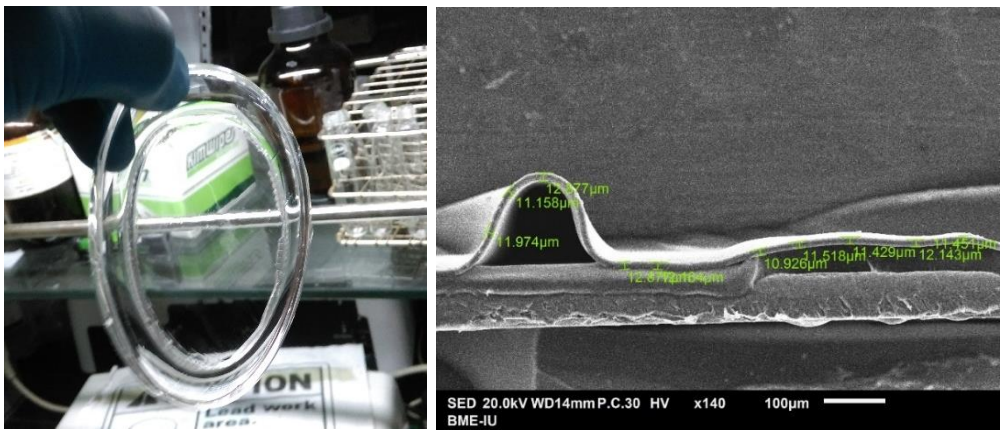

Figure 14: A spin-coated PDMS membrane (left) attached to a PDMS ring and its SEM image with thickness measurements (right).

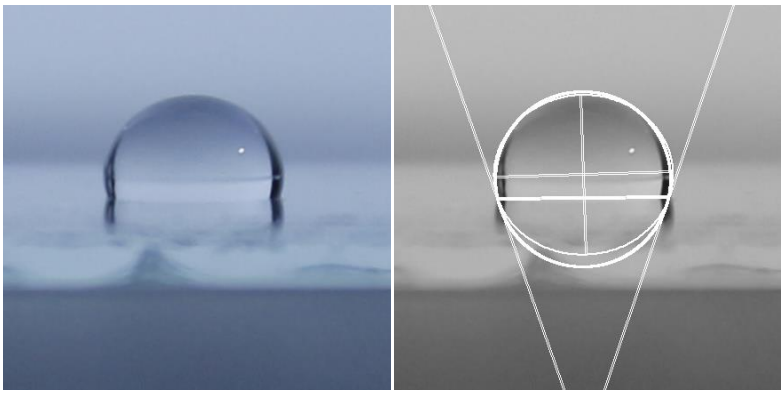

Figure 15: 10µL distilled water droplet on PDMS surface (left) and its contact angle measurement by the ImageJ software (right).

The contact angle created by the PDMS membrane and sessile water droplets was estimated to approximate 106^{o} ($\pm 1^{o}$), which is similar to the results reported in the literature [13][16] and confirms the hydrophobicity of PDMS surface.

This is the average value of five different measurements. Each measurement was conducted with a different PDMS sample and a new water droplet. Figure 15 is the image of a 10µL water droplet sitting on the PDMS membrane and the contact angle analyzed by Contact Angle plug-in of ImageJ image processing software.

4.3. AC & DC comparison

As expected from previous literature, the AC electric potential in this work demonstrated a better performance than that of both DC configurations. Applying the 275V, 1kHz driving signal could move droplets of 50X TAE reliably at the speed of approximately 1mm/s. On the other hand, in the DC configurations where 275VDC and inverse 275VDC were used, the droplets was movable but the movement was more sluggish and sometimes discontinuous. In these DC configurations, droplets of 50X TAE could be successfully actuated for the first few steps only. When more applications of DC electric potential were carried out, droplets tend to slow down and suffered from abnormal behaviors, which made droplet motion difficult to be controlled (see more in the Appendices). The cause of the phenomenon has not been fully investigated yet, nevertheless, the charge-trapping effect in the dielectric layer could suspiciously be attributed to this failure [12][13]. Under other circumstances, when compared to the AC electric potential, the speed of droplet motion induced by both DC configurations was lower, which makes the AC driving signal the best selection.

The results from this comparison confirms the advantages of AC electric potential in droplet manipulation as reported from earlier literature. This finding can be helpful in determining which method of actuation should be chosen for a reliable performance of the DMF system in the future.

4.4. Droplet operations

The operations below were accomplished using the AC driving signal (275V, 1kHz) and droplets of 50X TAE solution mixed with food-coloring dyes. PDMS membrane was used as the dielectric layer and peanut oil was selected for medium filler.

Droplet transportation. The current setup of the system was capable of transporting unit-size droplets of a minimum volume of 3.5µL. The volume was estimated by multiplying the electrode area by the gap height (9 mm^2 x 0.381 mm spacer). Droplets of 50X TAE solution started to move at the minimum voltage of approximate 120V and could be moved reliably at the speed of roughly 1mm/s with 275V driving signal. The movement was continuous, and droplets could move through all electrodes and in any direction such as forward, backward, to the left or to the right. The speed was estimated by determining the transit time Δt for the droplet to reach and cover a whole electrode following the activation of that electrode and then, dividing the distance between two electrodes by this Δt value. Figure 16 below demonstrates a droplet transportation sequence.

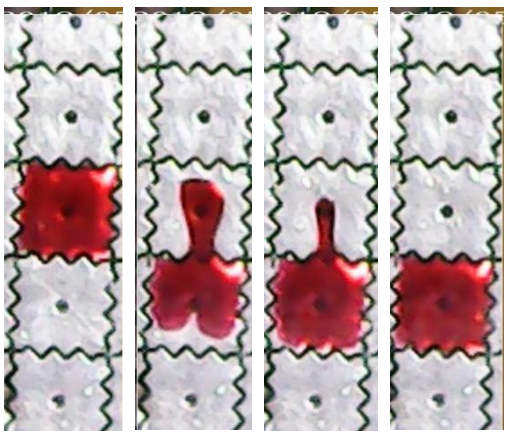

Figure 16: Transportation operation of a 50X TAE droplet mixed with red food dye.

The threshold actuation voltage was determined by gradually lowering the applied voltage from 275V to 60V (which is the minimum operating voltage of the HV507) and then increasing it back to 275V during transportation of droplets. The point where droplets started to move after immobilization was identified as the threshold voltage. Droplets moved sluggishly under 120V application and their speeds increased with the increase in applied voltage levels, as described in Figure 17 below.

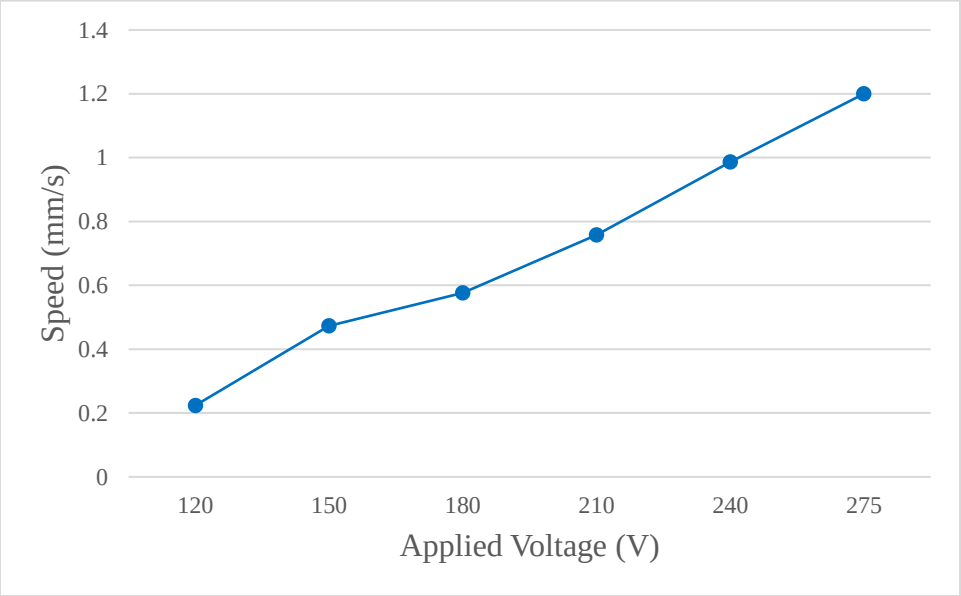

Figure 17: Speed of 50X TAE droplets vs AC voltage values (1kHz).

Droplet dispense. Steps of droplet dispense operation are illustrated in the Figure 18 below. A reservoir was holding 20µL of 50X TAE solution mixed with red food dye while a liquid protrusion extended from the reservoir due to a path of energized electrodes adjacent to the source. Turing off one electrode in the middle of the liquid finger caused the liquid drawn toward the reservoir and the terminal one, which were kept energized at that moment. The result was that the liquid finger broke in the middle and a new droplet with the unit-size volume of 3.5µL was then generated on the terminal electrode.

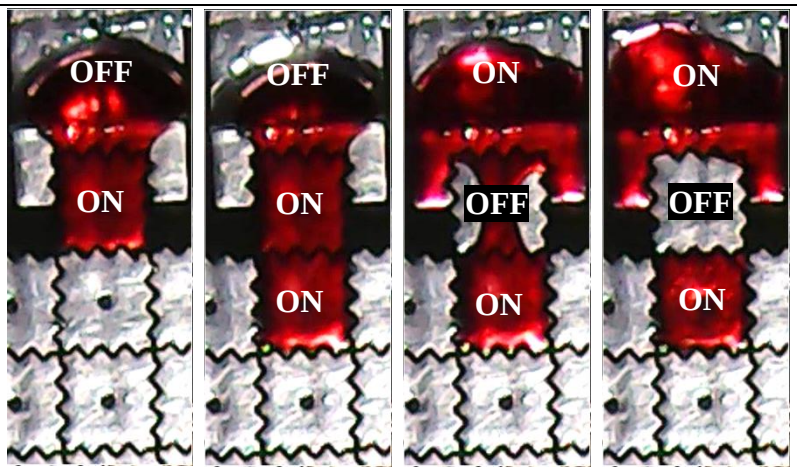

Figure 18: Dispense operation of a unit-size droplet from a reservoir.

Droplet mixing. Figure 19, 20 below show the mixing operation of two droplets of 50X TAE solution. One droplet was mixed with the green food dye and the other was mixed with the yellow one. Figure 19 demonstrates the moment when the two droplets were brought together and merged into a single double-size droplet. Mixing process was initiated by transporting the double-size droplet with a pair of energized electrodes, which is known as double-actuation in this report, so that the entire droplet body was controlled. The merged droplet was circulated in a loop pattern and the recirculating flow [17] occurring inside the droplet during transportation helped speed up mixing process.

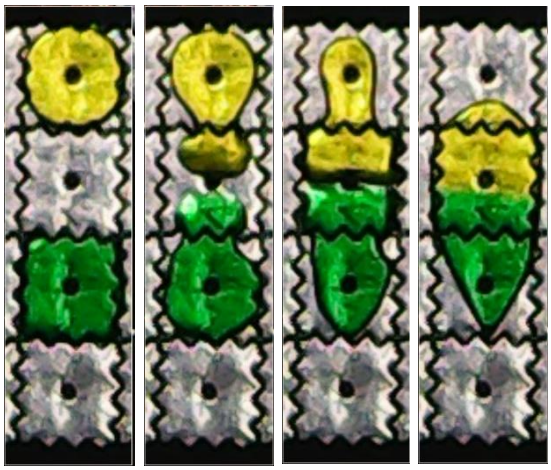

Figure 19: Two unit-size droplets were merged into a single double-size droplet.

The final result was that two droplets were mixed together and a change in droplet color could be observed in Figure 20. Two droplets used in the experiment was 3.5µL each and was introduced into the DMF system via droplet dispense operation.

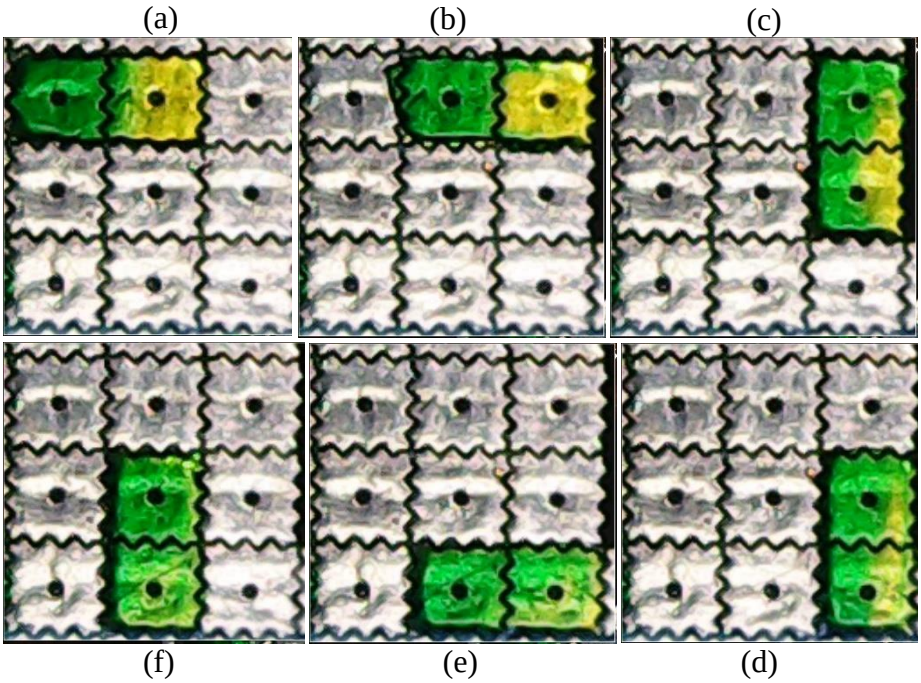

Figure 20: Once merged, the double-size droplet was manipulated by double actuation and moved in a circular pattern to speed up mixing.

Droplet splitting. After being merged and mixed, a double-size droplet should be separated back into two smaller droplets or children droplets which could be manipulated by a single electrode in other operations. Figure 21 describes a double-size droplet being split in a linear path three control electrodes. The bottom electrode was always kept energized while the two upper ones were activated sequentially, drawing the liquid upward and necking in the middle of the droplet. The result was that one double-size droplet was divided into two smaller droplets. However, in this splitting sequence, two split droplets were observed to have different volume, which could cause the droplet with less volume unable to be transported in the next step. Therefore, another method of splitting was also tried out in the Figure 22, in which a double-size droplet

was elongated and divided in a diagonal path. It was observed that droplets split by this method may be more equal in volume, even though the volume could not be the same. They are, however, still observations and therefore more investigation and development is mandatory in order to achieve a splitting operation with more exact volume control.

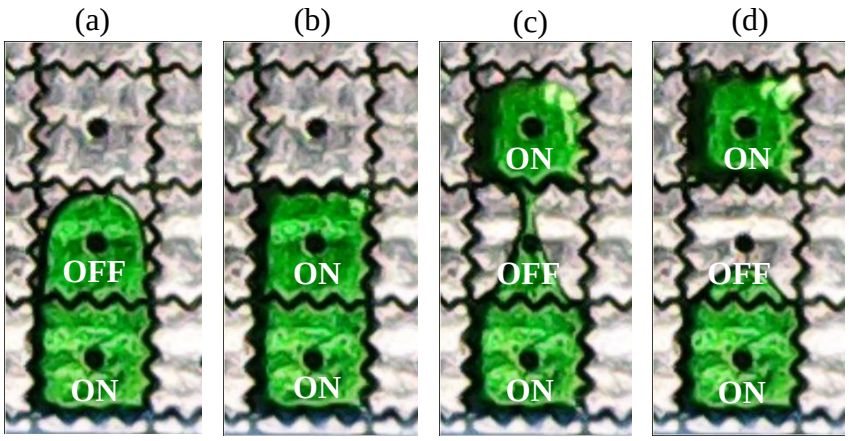

Figure 21: A double-size droplet was split into two smaller droplets in a linear path.

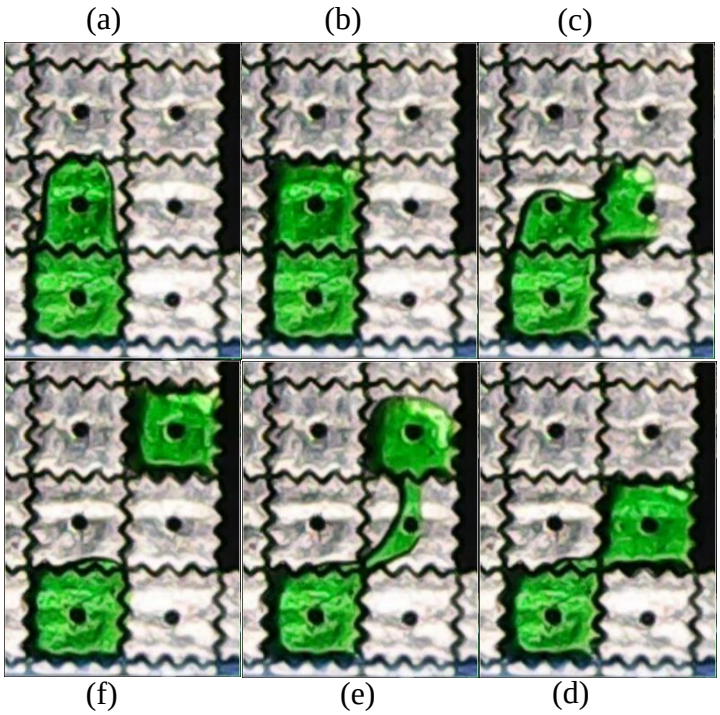

Figure 22: A double-size droplet was split into two smaller droplets in a diagonal path.

4.5. Actuation of protein droplets

In this experiment, droplets of protein solution of three different concentrations including 1.25 mg.mL^{-1}, 2.5 mg.mL^{-1} and 5 mg.mL^{-1} were tested on the fabricated DMF system. There was no evidence of the protein adsorption existing in all experiments carried out. Droplets of all three concentrations could successfully be introduced into the active area of the electrode array by the dispense operation. 20µL of each solution was pipetted into a reservoir using a 2-20µL Eppendorf pipette and unit-size droplets of protein solutions were drawn from the reservoirs and manipulated by the regular transportation sequence using 275V, 1kHz driving signal. No occlusion was observed during the dispense and transportation of all droplets; nevertheless there was a decrease in transportation speed when droplets of more concentrated protein solutions were actuated, as illustrated in Figure 23 below. The cause of this reduction could be attributed to the higher viscosity of solutions containing more protein concentration. The results from this experiment, in general , confirmed the effectiveness of medium-filling peanut oil in suppressing biofouling and enabling motion of droplets that contain proteins or biomolecules.

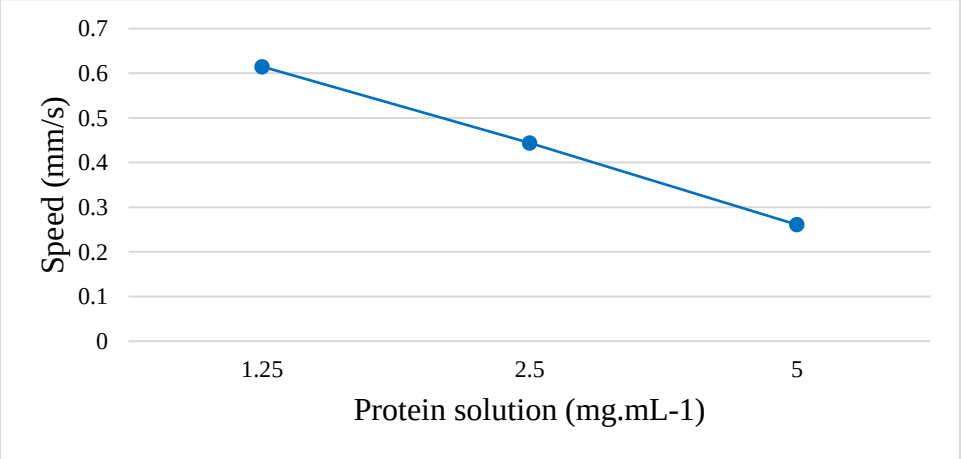

Figure 23: Droplet speed versus protein concentration.

4.6. DMF-based Recombinase Polymerase Amplification (RPA)

Unfortunately, this experiment failed to complete due to the immobilization of the Master mix droplets even though the droplet of DNA and Magnesium Acetate could be transported without any problem as in other experiments described in this report. Figure 24 below illustrates the behavior of two types of droplet.

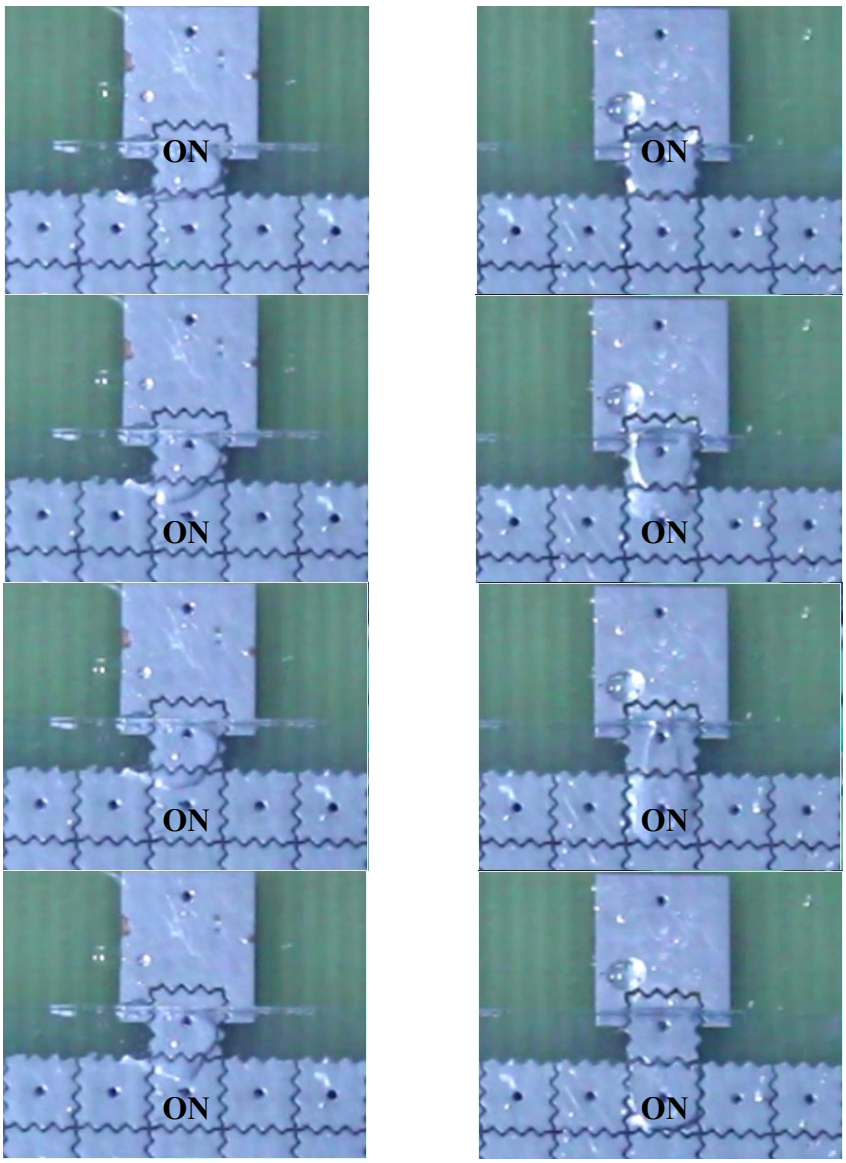

Figure 24: Movement of two types of droplet: Master mix (left) and mixture of DNA and Magnesium Acetate (right). The Master mix droplet tried to reach the ON electrode but the movement was not possible while on the right the droplet could move without any problem.

The result of the experiment was actually expected before since the Master mix exhibited much higher viscosity than the protein solutions that had been used in the previous experiments. Because there had been a decrease in droplet speed observed when there was an increase in protein concentration, i.e. an increase in liquid viscosity, the viscosity of the Master mix droplet might have exceeded the limit of the actuation force of the current DMF system in this case. It could be seen clearly that the Master mix droplet tried to reach to the energized electrode by protruding a "liquid tail"; however, its viscosity was too high for the actuation force to overcome and therefore, the droplet could only swirl its liquid tail instead of moving towards the activated electrode. Even when the top plate was elevated from the bottom one by one more layer of electrical tape (4 layers in total) in order to reduce the pressure inside the gap, the Master mix droplet could not move either. On the other hand, from the next input site, the droplet of DNA and Magnesium Acetate mixture could be transported without any problem for several cycles. However, when the droplet was moved towards and merged with the Master mix droplet which was being pinned down at its input site, movement was no longer possible. As a consequence, this experiment was not completed.

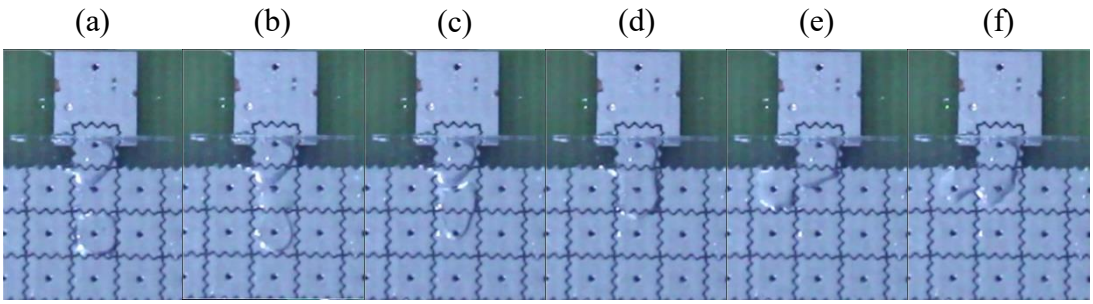

Figure 25: (a - d) Droplet of DNA and Magnesium Acetate mixture (lower) was moved and merged with the Master mix droplet (upper) stuck at its input site. (e) and (f) The behavior of the merged droplet under activation of some neighboring electrodes. Liquid protrusion was seen but no complete movement was obtained.

CHAPTER V: DISCUSSION

5.1. Limitations of the current system

So far, even though the Digital Microfluidic (DMF) system fabricated in this work has been capable of performing basic and simple droplet operations such as dispense, transportation, mixing and splitting, the device is still suffering from several limitations that restrict its performance and reliability.

PDMS used in this study is an attractive alternative for fabricating dielectric and hydrophobic layers in terms of cost and availability. Compared with PE plastic film and Rain-X water repellant coating used in the pre-thesis work, PDMS exhibited a higher dielectric constant, better hydrophobicity, more durability and reproducibility by allowing a single spin-coated membrane to be used multiple times. However, for more complex DMF-based applications, PDMS turned out to not be an appropriate choice due to its inadequacy of actuation performance. PDMS has a dielectric constant of 2.7 [11] which can be considered moderate among polymeric materials. However, it seems to be fairly low when compared to values of other materials commonly used for dielectric layer such as Parylene-C (3.15) or SiO_2 (3.9) [55]. Under the same parameters of voltage and thickness, lower dielectric constant results in lower actuation force and therefore, lower speed of droplet motion. Moreover, the sticky nature of cross-linked PDMS surface further contributes to resistance force and hinders droplet motion. Peanut oil can overcome high contact angle hysteresis of PDMS surface; however, its high viscosity still causes a minimal negative effect on droplet motion. On the other hand, droplet speed can be enhanced by either thinning the PDMS membrane or using higher voltages. With the use of a DIY (do-it-yourself) spin coater, which has the

maximum rotational speed restricted to 3000 rpm/m, the minimum thickness of PDMS membrane produced was approximately 11µm, which is much thicker than 1-2µm insulators in other literature. Much thinner membrane could be achievable by diluting PDMS emulsions in hexane before spinning; however, such thin membranes are more susceptible to wrinkle and tear during separation and handling by hands. Thicker insulating layer means lower effective capacitance, according to the parallel-plate capacitor equation, and therefore further reduces the actuation force. This leaves us with the second option of using higher voltages. Nevertheless, increasing actuation voltage puts the system at the risk of dielectric breakdown, especially when PDMS has a dielectric strength of approximately 19 V/µm [11] or 21.2 V/µm [55], which is considerably low when compared to other materials commonly used for insulating such as Parylene-C (268 V/µm) or SiO_2 (400-600 V/µm) [55]. Due to all reasons mentioned above, even though the actuation voltage has been increased to upper limits of PDMS membrane and electronic components, droplet motion was not as good as other literature where droplets can move at a speed of tens or even hundreds of mm/s.

The insufficiency of actuation force of the current system results in slow droplet movements, which in turns reduce the efficiency of mixing operation that mostly depends on the recirculating flows inside droplets during transportation to speed up mixing process. In addition, the methods that were used currently to perform the splitting and dispense operations are still simple and do not provide a way to quantitatively control droplets. So far, the volume of droplets generated in dispense operation was just estimated by the volume created by the top and bottom plates over an occupied electrode, which can be more or less than the real volume of droplets. During splitting operation, two smaller droplets could be formed after a random break

along the neck of the liquid column, leading to an asymmetric splitting process instead of a symmetric one. The situation might get worse when one of the two split droplets did not have enough volume to be actuated on the next move. As a consequence, further investigation and development are mandatory so that the operations can be more quantitatively controllable and accurate, which are essential for more complex applications.

In the RPA assay, the situation became even worse when the inadequacy of actuation force resulted in the immobilization of the Master mix droplet due to its high viscosity and ultimately lead to the failure of the entire experiment. That was also during the experiment of RPA that another limitation of the current device was realized. Generally, unit-size droplets can be introduced into the system via the dispense operation from the reservoirs where larger volumes of reagents are stored. However, in some cases such as the RPA assay in this study, where the amount of reagents was limited and therefore, manual dispense of required volumes by pipettes directly onto the electrode arrays are usually employed before the top plate is installed. This can be done easily in air medium; nevertheless, doing so with oil-filled systems may raise the risk of oil spilling or droplet slipped from its initial position when the top plate is lower down. With that reason, it is beneficial to come up with another method such as an actuating electrode serving as an input site by which unit-size droplets or low-volume reagents can be dispensed directly into the system using no reservoirs.

The unreliable and obstructive movement of droplets in this study is also partially ascribed to the imperfections on the fabricated hydrophobic surface. It is known that a smooth surface is essential for easy and reliable droplet motion. However, due to the amateur performance of the DIY spin-coater and lacking in clean room

conditions, surface flaws such as dust or tiny cavities, were inevitable during the fabrication process of the micro-thin PDMS membranes. Dust that was stuck in the membranes increased the surface roughness and hindered droplet motion while tiny cavities created weak spots on the membrane where dielectric breakdown could happen easily.

5.2. Future plan

From the experience learned from this work, a plan for a next version of the DMF system has already been set up. In order to improve the performance of the next device, a combination of PVDF (polyvinylidene difluoride) [70][71] and Fluoropel PFC-1601V (Cytonix, USA) will be employed for dielectric and hydrophobic coatings. PVDF has a much higher dielectric constant (around 10) and dielectric strength (roughly 600 V/µm) than those of PDMS while Fluoropel PFC-1601V [72] can provide a hydrophobic fluoropolymer coating similar to the Teflon AF1600 at a lower cost. With the use of Fluoropel for hydrophobic coating, we can use the silicone oil 1Cst, which is less viscous than peanut oil, for medium filler and therefore, the speed of droplet motion can be significantly enhanced. This scheme would be beneficial in a way that reliable droplet motion is the basics for other more complex operations.

The improvement of the next version also comes from the enrichment in system features including larger electrode arrays so that there is enough space for multiple-step protocols, heating chamber embedded inside the electrode panel to enhance heating efficiency, sensing and compensation system by which the actuation force acting on droplets will be monitored and maintained to ensure reliable droplet movements, and obviously a better user interface that is more user-friendly and contains more functions besides real-time manual control of droplet movements such as running

a user-predefined sequence of transportation or moving a droplet using an auto-routing path. Electronic control, including both setting and reading, for voltage level and frequency and isolation of high voltage from other electronic components are also valuable features that should be considered.

CHAPTER VI: CONCLUSION

In this study, an investigation on the design and fabrication of a Digital Microfluidic system, intentionally used for Nucleic Acid Amplification Tests, has been carried out. The implemented DMF system consists of four main components: a controller board integrated with a high-voltage power converter which can supply up to 275VDC from a 12VDC input, an electrode array fabricated on a PCB panel and containing a total number of 63 usable electrodes, a foil carrier used for carrying the insulating layer and finally, an ITO glass slide as the top counter electrode. A heating unit was integrated underneath the electrode panel to provide incubation temperature. PDMS, thanks to its moderate dielectric constant (ε_r = 2.7) and very good hydrophobicity, was chosen as the material for fabricating the dielectric layer. No additional hydrophobic treatment was used in the research. A home-made spin coater and Petri dishes were exploited to create PDMS membranes with an average thickness of 11µm. Contact angle measurements revealed an average value of 106^o between 10µL droplets of distilled water and the PDMS surface. Peanut oil was used for the medium filler. The fabricated device was verified to be capable of performing all four droplet operations. An approximately 3.5µL droplet of 50X TAE solution was successfully dispensed from a 20µL reservoir and then transported continuously at a maximum speed of 1mm/s using 275V, 1kHz driving signal. Using the same experimental parameters, a single double-size droplet could be formed by mixing two unit-size droplets together and then, could be split back into two smaller droplets; nevertheless, a more controllable splitting process may need more investigation. Moreover, the device was able to work with droplets of BSA protein solutions thanks to the use of oil-filled medium. An RPA assay was also designed to run on the presented system;

however, the result of this experiment was a failure because the Master mix was too viscous for the current system to actuate. So far, the function of the fabricated DMF device is limited to simple and distinct operations due to inadequate performance of PDMS as both dielectric and hydrophobic layers. Even though, this may be an attractive method due to its inexpensiveness and accessibility, real clinical applications demand much more than that and this raises a necessity for a significant upgrade in all aspects of the next DMF system including performance, reliability, controllability and functionality.

REFERENCES

[1] K. Choi, A. H. C. Ng, R. Fobel, and A. R. Wheeler, "Digital Microfluidics," *Annu. Rev. Anal. Chem.*, vol. 5, no. 1, pp. 413–440, 2012.

[2] B. Coelho *et al.*, "Digital Microfluidics for Nucleic Acid Amplification," *Sensors*, vol. 17, no. 7, p. 1495, 2017.

[3] B. Coelho *et al.*, "A Digital Microfluidics Platform for Loop-Mediated Isothermal Amplification Detection," *Sensors*, vol. 17, no. 11, p. 2616, 2017.

[4] L. Wan *et al.*, "A digital microfluidic system for loop-mediated isothermal amplification and sequence specific pathogen detection," *Sci. Rep.*, vol. 7, no. 1, pp. 1–11, 2017.

[5] M. Alistar and U. Gaudenz, "OpenDrop: An Integrated Do-It-Yourself Platform for Personal Use of Biochips," *Bioengineering*, vol. 4, no. 2, p. 45, 2017.

[6] M. Louie, L. Louie, and A. E. Simor, "The role of DNA amplification technology in the diagnosis of infectious diseases.," *CMAJ*, vol. 163, no. 3, pp. 301–9, Aug. 2000.

[7] "WHO | Antimicrobial resistance," *WHO*, 2018. [Online]. Available: http://www.who.int/antimicrobial-resistance/en/. [Accessed: 07-Jul-2018].

[8] H. Norian, R. M. Field, I. Kymissis, and K. L. Shepard, "An integrated CMOS quantitative-polymerase-chain-reaction lab-on-chip for point-of-care diagnostics," *Lab Chip*, vol. 14, no. 20, pp. 4076–4084, 2014.

[9] S. Kalsi *et al.*, "Rapid and sensitive detection of antibiotic resistance on a programmable digital microfluidic platform," *Lab Chip*, vol. 15, no. 14, pp.

3065–3075, 2015.

[10] Y. H. Chang, G. Bin Lee, F. C. Huang, Y. Y. Chen, and J. L. Lin, "Integrated polymerase chain reaction chips utilizing digital microfluidics," *Biomed. Microdevices*, vol. 8, no. 3, pp. 215–225, 2006.

[11] D. Corning, "Electronics Sylgard ® 184 Silicone Elastomer," *Prod. Datasheet*, pp. 1–3, 2013.

[12] S. Sohail, D. Das, S. Das, and K. Biswas, "Physics of Semiconductor Devices," pp. 7–10, 2014.

[13] G. Tabatabaeipour, H. Hajghassem, and M. MohtashamiFar, "Low-cost hydrophobic layer as a top plate in two-plate digital microfluidics," *Eur. Phys. J. Appl. Phys.*, vol. 71, no. 1, p. 11101, 2015.

[14] Y.-P. Zhao and Y. Wang, "Fundamentals and Applications of Electrowetting," *Rev. Adhes. Adhes.*, vol. 1, no. 1, pp. 114–174, 2013.

[15] Y. Yuan and T. R. Lee, *Contact Angle and Wetting Properties*. 2013.

[16] F. Mugele and J. C. Baret, "Electrowetting: From basics to applications," *J. Phys. Condens. Matter*, vol. 17, no. 28, 2005.

[17] S. K. Cho, H. Moon, and C.-J. Kim, "Creating, Transporting, Cutting, and Merging Liquid Droplets by Electrowetting-Based Actuation for Digital Microfluidic Circuits," *J. Microelectromechanical Syst.*, vol. 12, no. 1, pp. 70–80, 2003.

[18] M. K. Chaudhury and G. M. Whitesides, "How to make water run uphill," *Science (80-.).*, vol. 256, no. 5063, pp. 1539–1541, 1992.

[19] T. Ruo and S. Ecs, "References and Notes 1.," vol. 321, no. August, pp. 652–653, 2008.

[20] K. Ichimura, S. K. Oh, and M. Nakagawa, "Light-driven motion of liquids on a photoresponsive surface," *Science (80-.).*, vol. 288, no. 5471, pp. 1624–1626, 2000.

[21] M. A. Burns *et al.*, "Microfabricated structures for integrated DNA analysis," *Proc. Natl. Acad. Sci. U. S. A.*, vol. 93, no. 11, pp. 5556–61, 1996.

[22] D. T. Burke, M. A. Burns, and C. Mastrangelo, "Microfabrication technologies for integrated nucleic acid analysis," *Genome Res.*, vol. 7, no. 3, pp. 189–197, 1997.

[23] T. S. Sammarco and M. A. Burns, "Thermocapillary pumping of discrete drops in microfabricated analysis devices," *AIChE J.*, vol. 45, no. 2, pp. 350–366, 1999.

[24] T. S. Sammarco and M. A. Burns, "Heat-transfer analysis of microfabricated thermocapillary pumping and reaction devices," *J. Micromechanics Microengineering*, vol. 10, no. 1, pp. 42–55, 2000.

[25] Z. Guttenberg *et al.*, "Planar chip device for PCR and hybridization with surface acoustic wave pump," *Lab Chip*, vol. 5, no. 3, pp. 308–317, 2005.

[26] A. Renaudin, P. Tabourier, J. C. Camart, and C. Druon, "Surface acoustic wave two-dimensional transport and location of microdroplets using echo signal," *J. Appl. Phys.*, vol. 100, no. 11, pp. 65–68, 2006.

[27] A. Renaudin, J. P. Sozanski, B. Verbeke, V. Zhang, P. Tabourier, and C. Druon, "Monitoring SAW-actuated microdroplets in view of biological applications,"

Sensors Actuators, B Chem., vol. 138, no. 1, pp. 374–382, 2009.

[28] A. L. Zhang, Z. Q. Wu, and X. H. Xia, "Transportation and mixing of droplets by surface acoustic wave," *Talanta*, vol. 84, no. 2, pp. 293–297, 2011.

[29] J. Reboud *et al.*, "Shaping acoustic fields as a toolset for microfluidic manipulations in diagnostic technologies.," *Proc. Natl. Acad. Sci. U. S. A.*, vol. 109, no. 38, pp. 15162–7, Sep. 2012.

[30] N. T. Nguyen, K. M. Ng, and X. Huang, "Manipulation of ferrofluid droplets using planar coils," *Appl. Phys. Lett.*, vol. 89, no. 5, pp. 2006–2009, 2006.

[31] U. Lehmann, S. Hadjidj, V. K. Parashar, C. Vandevyver, A. Rida, and M. A. M. Gijs, "Two-dimensional magnetic manipulation of microdroplets on a chip as a platform for bioanalytical applications," *Sensors Actuators, B Chem.*, vol. 117, no. 2, pp. 457–463, 2006.

[32] A. Beyzavi and N.-T. Nguyen, "One-dimensional actuation of a ferrofluid droplet by planar microcoils," *J. Phys. D. Appl. Phys.*, vol. 42, no. 1, p. 015004, 2009.

[33] Y. Zhang and N. T. Nguyen, "Magnetic digital microfluidics - a review," *Lab Chip*, vol. 17, no. 6, pp. 994–1008, 2017.

[34] P. R. C. Gascoyne *et al.*, "Dielectrophoresis-based programmable fluidic processors," *Lab Chip*, vol. 4, no. 4, pp. 299–309, 2004.

[35] J. L. Jackel, S. Hackwood, and G. Beni, "Electrowetting optical switch," *Appl. Phys. Lett.*, vol. 40, no. 1, pp. 4–6, 1982.

[36] J. L. J. Lee and C.-J. C. Kim, "Liquid Micromotor Driven by Continuous

Electrowetting," *Proc. MEMS 98. IEEE. Elev. Annu. Int. Work. Micro Electro Mech. Syst. An Investig. Micro Struct. Sensors, Actuators, Mach. Syst. (Cat. No.98CH36176*, pp. 538–543, 1998.

[37] M. G. Pollack, R. B. Fair, and A. D. Shenderov, "Electrowetting-based actuation of liquid droplets for microfluidic applications," *Appl. Phys. Lett.*, vol. 77, no. 11, pp. 1725–1726, 2000.

[38] M. G. Pollack, "Electrowetting-based microactuation of droplets for digital microfluidics," pp. 1–159, 2001.

[39] J. Lee, H. Moon, J. Fowler, T. Schoellhammer, and C. J. Kim, "Electrowetting and electrowetting-on-dielectric for microscale liquid handling," *Sensors Actuators, A Phys.*, vol. 95, no. 2–3, pp. 259–268, 2002.

[40] M. G. Pollack, A. D. Shenderov, and R. B. Fair, "Electrowetting-based actuation of droplets for integrated microfluidicsElectronic supplementary information (ESI) available: six videos showing droplet flow, droplet dispensing and electrowetting. See http://www.rsc.org/suppdata/lc/b1/b110474h/," *Lab Chip*, vol. 2, no. 2, p. 96, 2002.

[41] J. Gong and C.-J. "CJ" Kim, "All-electronic droplet generation on-chip with real-time feedback control for EWOD digital microfluidics," *Lab Chip*, vol. 8, no. 6, p. 898, 2008.

[42] M. Vallet, B. Berge, and L. Vovelle, "Electrowetting of water and aqueous solutions on poly(ethylene terephthalate) insulating films," *Polymer (Guildf).*, vol. 37, no. 12, pp. 2465–2470, 1996.

[43] T. B. Jones, J. D. Fowler, Y. S. Chang, and C. J. Kim, "Frequency-based

relationship of electrowetting and dielectrophoretic liquid microactuation," *Langmuir*, vol. 19, no. 18, pp. 7646–7651, 2003.

[44] T. B. Jones, K. L. Wang, and D. J. Yao, "Frequency-dependent electromechanics of aqueous liquids: Electrowetting and dielectrophoresis," *Langmuir*, vol. 20, no. 7. pp. 2813–2818, 2004.

[45] D. Chatterjee, H. Shepherd, and R. L. Garrell, "Electromechanical model for actuating liquids in a two-plate droplet microfluidic device," *Lab Chip*, vol. 9, no. 9, p. 1219, 2009.

[46] Y. Li, R. Chen, and R. J. Baker, "A fast fabricating electro-wetting platform to implement large droplet manipulation," *Midwest Symp. Circuits Syst.*, pp. 326–329, 2014.

[47] M. Abdelgawad and A. R. Wheeler, "Low-cost, rapid-prototyping of digital microfluidics devices," *Microfluid. Nanofluidics*, vol. 4, no. 4, pp. 349–355, 2008.

[48] D. Caputo, G. De Cesare, N. Lo Vecchio, A. Nascetti, E. Parisi, and R. Scipinotti, "Polydimethylsiloxane material as hydrophobic and insulating layer in electrowetting-on-dielectric systems," *Microelectronics J.*, vol. 45, no. 12, pp. 1684–1690, 2014.

[49] M. Abdelgawad and A. R. Wheeler, "Rapid prototyping in copper substrates for digital microfluidics," *Adv. Mater.*, vol. 19, no. 1, pp. 133–137, 2007.

[50] U. C. Yi and C. J. Kim, "Characterization of electrowetting actuation on addressable single-side coplanar electrodes," *J. Micromechanics Microengineering*, vol. 16, no. 10, pp. 2053–2059, 2006.

[51] C. G. Cooney, C. Y. Chen, M. R. Emerling, A. Nadim, and J. D. Sterling, "Electrowetting droplet microfluidics on a single planar surface," *Microfluidics and Nanofluidics*, vol. 2, no. 5. pp. 435–446, 2006.

[52] I. Barbulovic-Nad, H. Yang, P. S. Park, and A. R. Wheeler, "Digital microfluidics for cell-based assays," *Lab Chip*, vol. 8, no. 4, pp. 519–526, 2008.

[53] I. Barbulovic-Nad, S. H. Au, and A. R. Wheeler, "A microfluidic platform for complete mammalian cell culture," *Lab Chip*, vol. 10, no. 12, pp. 1536–1542, 2010.

[54] S. H. Au, S. C. C. Shih, and A. R. Wheeler, "Integrated microbioreactor for culture and analysis of bacteria, algae and yeast," *Biomed. Microdevices*, vol. 13, no. 1, pp. 41–50, 2011.

[55] H. Liu, S. Dharmatilleke, D. K. Maurya, and A. A. O. Tay, "Dielectric materials for electrowetting-on-dielectric actuation," *Microsyst. Technol.*, vol. 16, no. 3, pp. 449–460, 2010.

[56] J. Y. Yoon and R. L. Garrell, "Preventing biomolecular adsorption in electrowetting-based biofluidic chips," *Anal. Chem.*, vol. 75, no. 19, pp. 5097–5102, 2003.

[57] A. R. Wheeler, H. Moon, C.-J. Kim, J. a Loo, and R. L. Garrell, "Electrowetting-based microfluidics for analysis of peptides and proteins by matrix-assisted laser desorption/ionization mass spectrometry.," *Anal. Chem.*, vol. 76, no. 16, pp. 4833–4838, 2004.

[58] V. Srinivasan, V. K. Pamula, and R. B. Fair, "An integrated digital microfluidic lab-on-a-chip for clinical diagnostics on human physiological fluids.," *Lab Chip*,

vol. 4, no. 4, pp. 310–315, 2004.

[59] J. Gong and C.-J. "Cj" Kim, "Two Dimensional Digital Microfluidic System By Multi-Layer Printed Circuit Board," *Ieee*, vol. 11, pp. 2693–700, 2005.

[60] A. Manuscript, D. T. D. Microfluidics, U. M. Printed, and C. Board, "NIH Public Access," *Vital Heal. Stat. Ser. 20 Data From Natl. Vitalstatistics Syst. Vital Heal. Stat 20 Data Natl Vital Sta*, vol. 17, no. 2, pp. 257–264, 2009.

[61] E. Lebrasseur *et al.*, "Two-dimensional electrostatic actuation of droplets using a single electrode panel and development of disposable plastic film card," *Sensors Actuators, A Phys.*, vol. 136, no. 1, pp. 358–366, 2007.

[62] H. Moon, S. K. Cho, R. L. Garrell, and C. J. Kim, "Low voltage electrowetting-on-dielectric," *J. Appl. Phys.*, vol. 92, no. 7, pp. 4080–4087, 2002.

[63] M. Bienia, C. Quilliet, and M. Vallade, "Modification of Drop Shape Controlled by Electrowetting," *Langmuir*, vol. 19, no. 22, pp. 9328–9333, 2003.

[64] A. N. Banerjee, S. Qian, and S. W. Joo, "High-speed droplet actuation on single-plate electrode arrays," *J. Colloid Interface Sci.*, vol. 362, no. 2, pp. 567–574, 2011.

[65] I. Nagiel and R. Fair, "AC Electrowetting Actuation of Droplets on a Digital Microfluidic Platform," pp. 1–13, 2007.

[66] R. Fobel, C. Fobel, and A. R. Wheeler, "DropBot: An open-source digital microfluidic control system with precise control of electrostatic driving force and instantaneous drop velocity measurement," *Appl. Phys. Lett.*, vol. 102, no. 19, 2013.

[67] Nick de Smith, "Nixie HV Switching PSU," 2016. [Online]. Available: http://desmith.net/NMdS/Electronics/NixiePSU.html. [Accessed: 22-Jan-2018].

[68] Supertex Inc., "64-Channel Serial to Parallel Converter With High Voltage Push-Pull Outputs," *HV507 datasheet*, no. DSFP-HV507, 1995.

[69] S. K. Chae, J. H. Ryoo, and S. H. Lee, "Thin and large free-standing PDMS membrane by using polystyrene Petri dish," *Biochip J.*, vol. 6, no. 2, pp. 184–190, 2012.

[70] M. F. Samad and A. Z. Kouzani, "Design and Analysis of a Low Actuation Voltage Electrowetting-on- dielectric Microvalve for Drug Delivery Applications," *36th Annu. Int. Conf. IEEE Eng. Med. Biol. Soc.*, pp. 4423–4426, 2014.

[71] M. F. Samad, A. Z. Kouzani, M. M. Rahman, K. Magniez, and A. Kaynak, "Design and Fabrication of an Electrode for Low-actuation-Voltage Electrowetting-on-Dielectric Devices," *Procedia Technol.*, vol. 20, no. July, pp. 20–25, 2015.

[72] "Hydrophobic Coating and Foil Materials – OpenDrop." [Online]. Available: http://www.gaudi.ch/OpenDrop/?p=142. [Accessed: 25-Jul-2018].

[73] T. Imager, I. Multimeter, and C. Scopemeter, "Test Tools Catalog," 2007.

[74] N. Nuraje, W. S. Khan, Y. Lei, M. Ceylan, and R. Asmatulu, "Superhydrophobic electrospun nanofibers," *J. Mater. Chem. A*, vol. 1, no. 6, pp. 1929–1946, 2013.

APPENDICES

1. Integrated heating unit

Figure 26 demonstrates the way used to investigate the real temperatures of the peanut oil layer during heating. A clamp stand was used to keep the thermocouple probe to just touch the peanut oil and the temperatures were read by the Fluke True RMS 87V Digital Multimeter (DMM). The basic accuracy of temperature measurement when the 80BK K-type thermocouple probe is used with Fluke 87V DMM can be either 2.2^{o}C or 2%, whichever higher [73]. A DSLR camera was used to record the heating process and the fluctuation in temperature was observed.

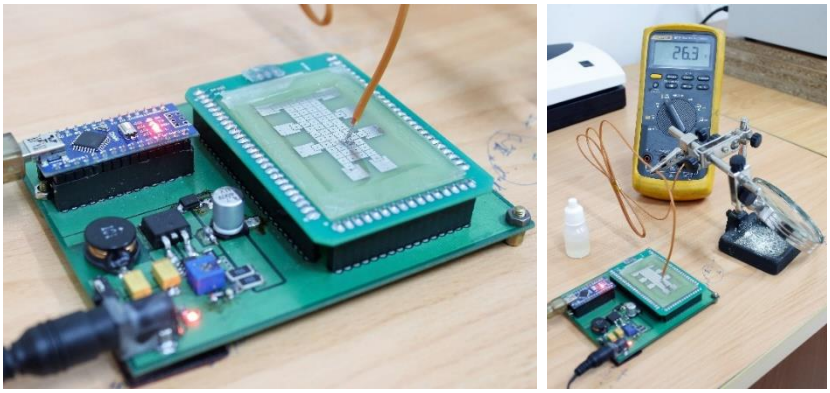

Figure 26: Set-up for investigating real temperature of peanut oil layer above the electrode panel during heating.

The temperature of the peanut oil can reach to the set point of 40^{o}C from 26^{o}C in an air-conditioning room within 7 minutes and 30 seconds. After that, the temperature was fluctuating around 40^{o}C with the maximum value of 41.1^{o}C and the lowest temperature of 38.1^{o}C, which was still well within the operating temperature range of the RPA assay that had been planned to run on the DMF device. The temperature could remain within the boundaries for more than 30 minutes, which was sufficient for the incubation time of the RPA assay.

2. DIY (Do-it-yourself) spin coater

In this thesis work, a spin coater was built for the fabrication of thin PDMS membranes. The spin coater was constructed from a 4-wire PC fan attached on a solid iron base to enhance stability. A 3D-printed non-vacuum chuck was held to the rotor of the fan by 4 screws and double-sided tape was used to stick the substrates to be coated onto the chuck before spinning. The entire system was placed and glued inside a plastic circular box for safety purposes. A driver shield that would fit the pinout of the Arduino Uno board was created to control the speed of the spin coater from the outside. A LCD screen displayed information about rotational speed and PWM control values. This DIY spin coater can reach to the maximum rotational speed of 3000 rpm/min, which is considerably low compared to other machines. Both single-step or two-step procedures can be performed using the DIY spin coater thanks to two in-built buttons of the device, one for setting the desired rotational speed and the other for running the rotor at the desired speed.

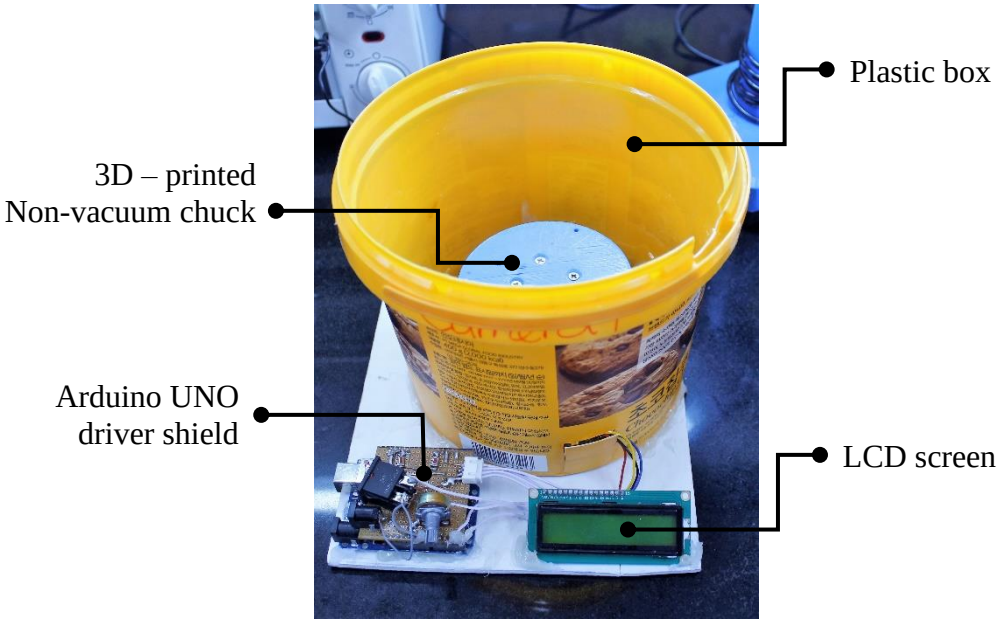

Figure 27: Do-it-yourself (DIY) spin coater for thin PDMS membrane fabrication.

The limitations of the current spin coater includes no timer, no vacuum chuck which would be more convenient and safer than using double-sided tape and no acceleration control which is also an important parameter in spinning procedures.

3. Windows User interface

In addition to the hardware, a user interface was also developed on Windows environment to provide a way for users to keep track of actuating electrodes as well as manipulating droplets directly via control options on the interface or from their keyboards. The program was developed using C# language and by Microsoft Visual Studio IDE. Below are some illustrations of the user interface and how it is used for the manipulation of droplets. An external DSLR camera was used to record the laptop screen when the user interface was being connected to the DMF system during droplet operations.

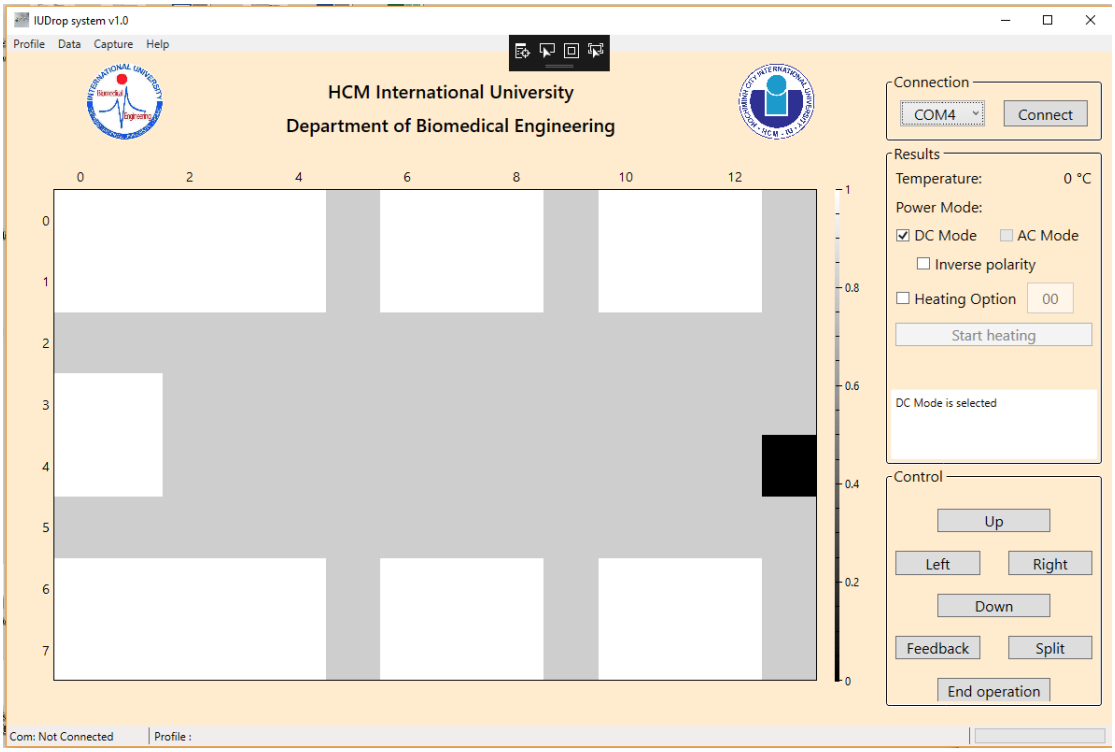

Figure 28: The user interface for manual manipulation of droplets.

Black color represents the energizing electrode

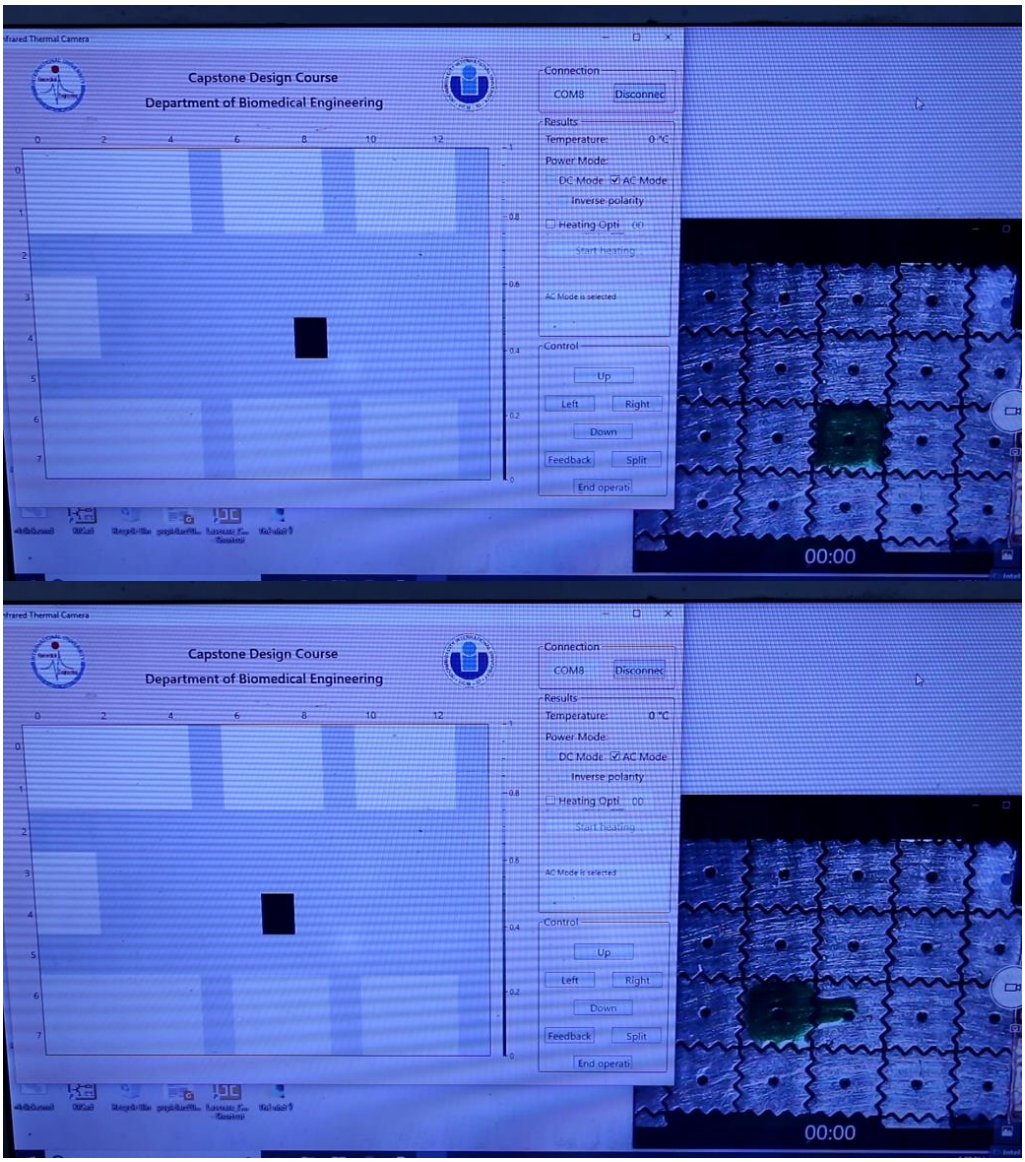

Figure 29: The user interface used with droplet transportation operation.

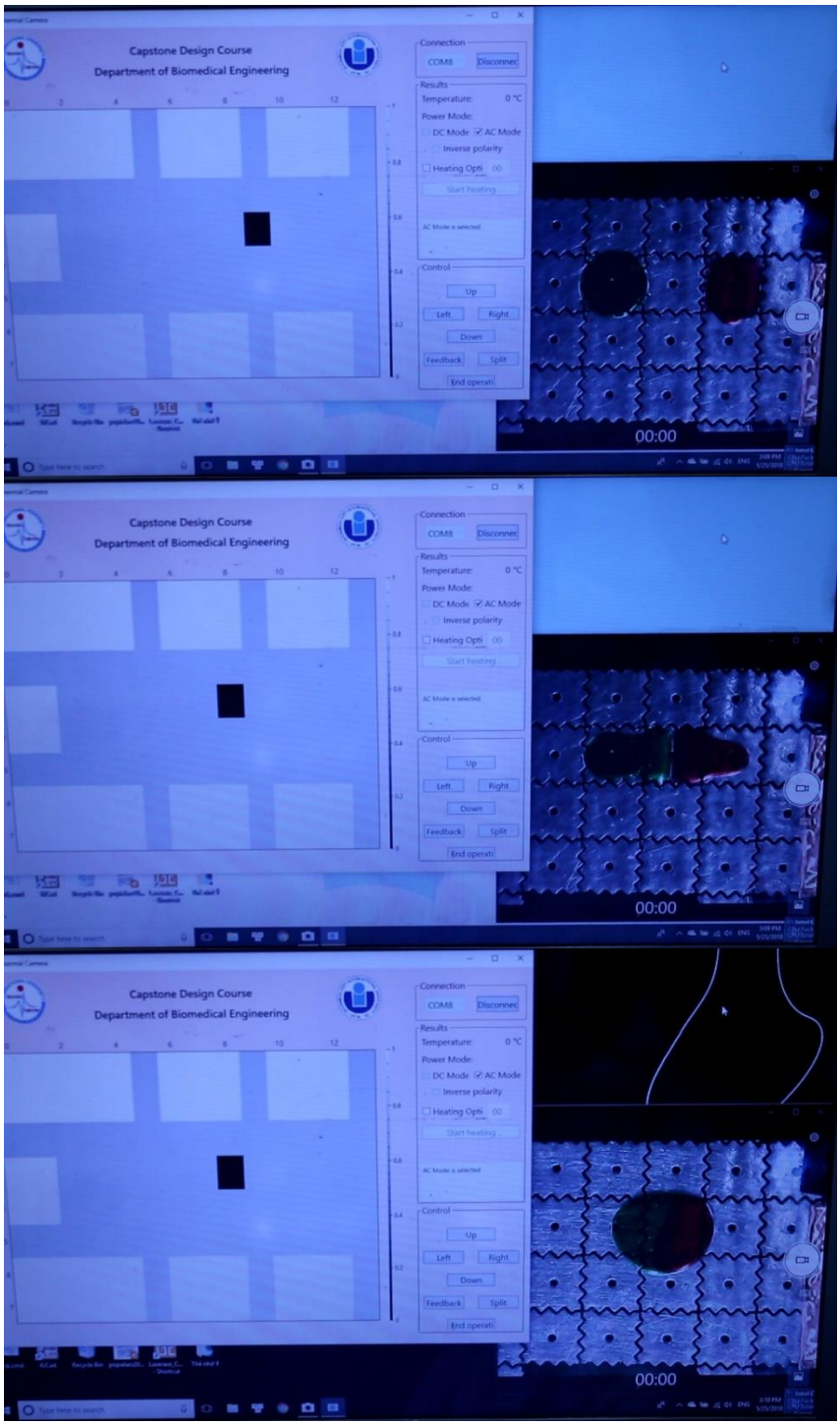

Figure 30: The user interface when used for droplet merging.

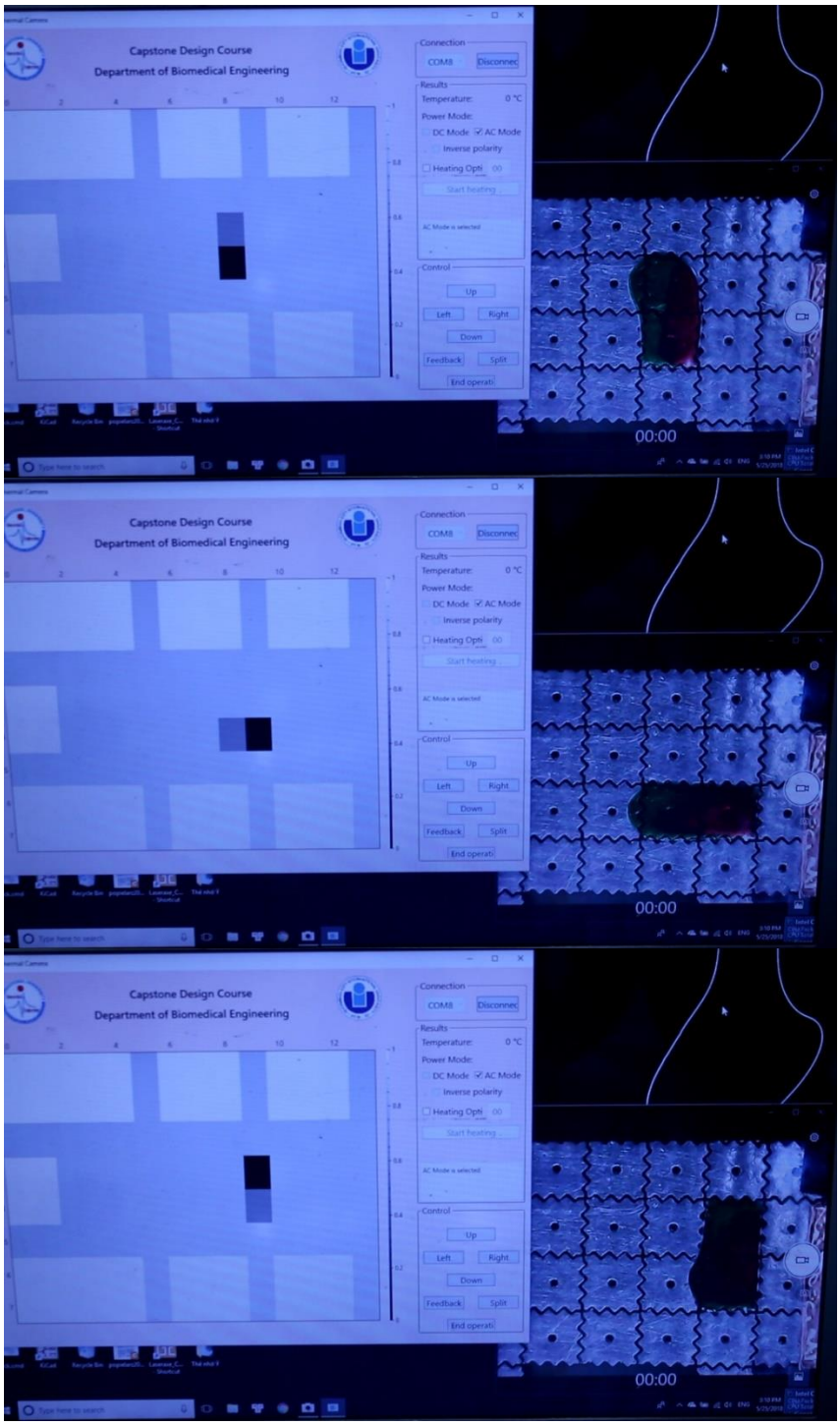

Figure 31: The user interface when double actuation used for mixing operation.

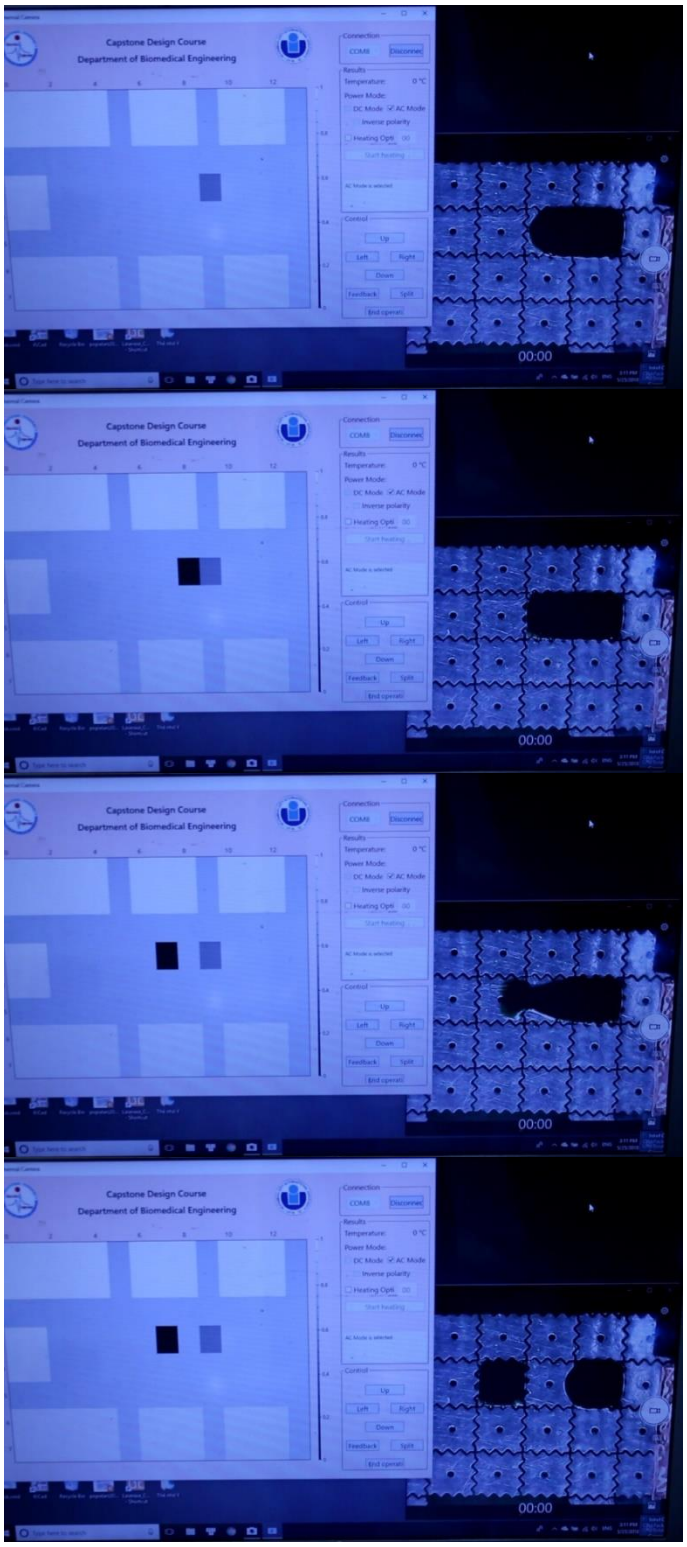

Figure 32: The user interface when used for droplet splitting operation.

4. AC & DC Comparison

As reported above, when the DMF system operated using the DC actuating configuration, liquid droplets could only be controlled for the first few steps and then, they suffered from abnormal behaviors such as vibration or swirling tails during transportation that made it more difficult to control their movement. Below are some footages of droplet abnormal behaviors that were observed.

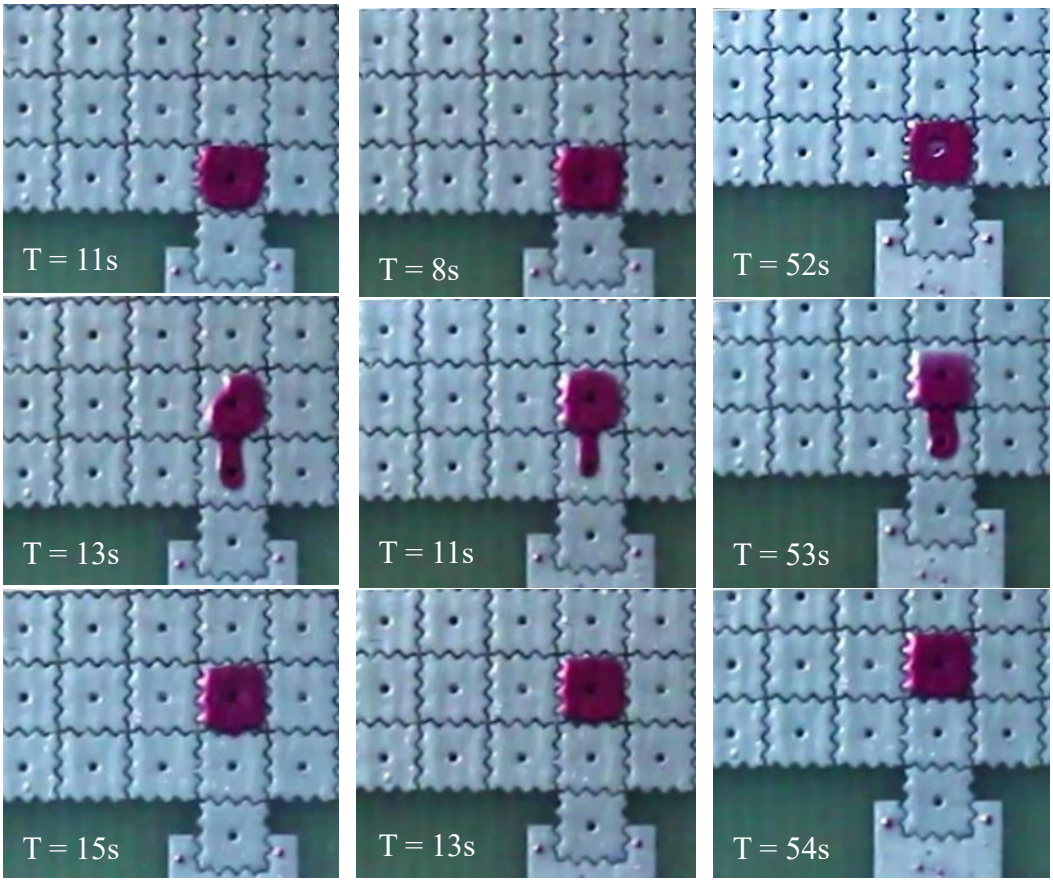

Figure 23: Droplet transportation using three actuating configuration: DC (left), inverse DC (middle) and AC (right). Both DC configurations have lower droplet speed than that induced by AC potential. (Δt_{DC} = 4s, $\Delta t_{inverse\ DC}$ = 5s and Δt_{AC} = 2s)

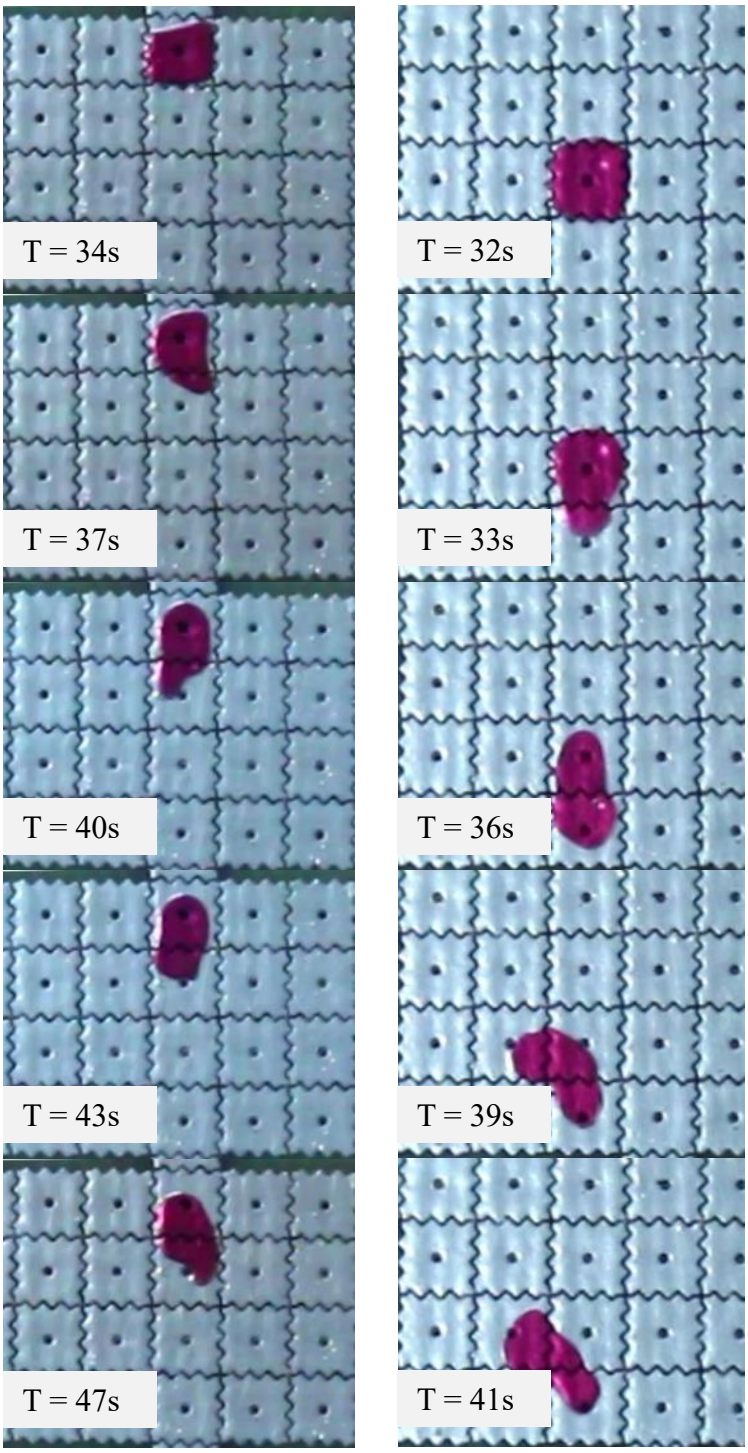

Figure 34: Abnormal behaviors of droplets under DC (left) and inverse DC (right). On the left, it took more than 13 seconds for the droplet to reach the activated electrode under DC potential. A swirling liquid tail appeared during movement. On the right, the droplet under inverse DC configuration was completely deviated from the activated electrode.